TU Delft

Simulations of Open Quantum Systems and Decoherence-Free Subspaces

Mark Weerheim, 4712927

Supervisors:	Dr. J.L.A. Dubbeldam
	Prof. Dr. Y.M. Blanter
Other committee members:	Dr. B. Janssens
	Dr. M. Blaauboer

Bachelor's Thesis
Applied Mathematics and Applied Physics
Delft University of Technology

To be defended on:
August 18th 2020
Faculties EEMCS and AS

Abstract

Complex quantum systems, such as a quantum computer, will always be coupled in some way to the environment. This can cause what's called *decoherence*, a destructive process by which information is lost from the system into the environment. In this bachelor thesis paper, we discuss decoherence-free subspaces within networks of coupled quantum harmonic oscillators (or QHOs). We investigate where such noiseless subspaces (or NSs) occur most frequently in an ensemble of Erdos-Renyi networks, for which we do not yet consider the influence of the bath. We then proceed by adding the bath into the equation, using some of the theory of open quantum systems. Specifically, we derive the Lindblad master equation and show its form for the case of our networks. Consequently, we simulate the behavior of the moments of the position operators for the graphs with 3 nodes, both by means of the full Lindblad equation, and by first tracing out those moments to obtain their differential equations. We compare those two results to each other, and also look back to the situation before adding the bath to see if the NSs are still present.

From the results of the simulations, we can conclude several things. Firstly, we see that for ensembles with probability of connection p very close to either 0 or 1, both to number of noiseless modes and the probability of finding at least one is largest. This is credited to their relatively high degrees of symmetry. Secondly, in the results of the density matrix and moment simulations, we see that, indeed, the noiseless modes are preserved when considering the influence of the bath. Furthermore, we can conclude that simulation of the density matrix for the case of coupled QHOs in a network is in many cases not stable; the cutoff at a finite level s needed to simulate an otherwise infinite-dimensional operator leads to non-positivity of the density matrix. Therefore, it is best to simulate the moments from their respective differential equations, as opposed to the full Lindblad master equation. Finally, the differential equations for the moments and their solutions show that there are indeed noiseless clusters for eigenmodes perpendicular to the center of mass, as predicted.

Contents

1 Introduction

Over the last few decades, the quantum computer has become an increasingly interesting topic, thanks to the prospect of quick factorization algorithms like Shor's algorithm [1]. But there are still some problems that must be overcome before quantum computers can be made [2], one of those being the problem of decoherence. Decoherence is (naturally) the loss of coherence which, in turn, is when different states in the system are in a definite phase relation to each other [3]. Normally, quantum systems evolve in a unitary way, but decoherence can cause the system (when viewed on its own) to evolve non-unitarily [4]. Decoherence happens when a quantum system is embedded within an environment, which is typically the case for all real applications. So our goal in this paper will be to investigate when such systems can stay coherent; specifically, we will investigate networks of coupled QHOs (quantum harmonic oscillators) which are embedded in a bath of infinitely many QHOs.

We will first look at the properties of a few simple networks of coupled QHOs, for which we consider the environment to act on each node identically, and use this approach to find in which type of network we can find such "noiseless clusters" the most abundantly. However, since realistic quantum systems always entail some form of dissipation when coupled to the environment, we need to look at these networks from the perspective of the theory of open quantum systems. What this means is that we will use the Lindblad master equation, which we will derive in the general case, and we will look at its form when applied to the networks that we want to investigate. We will then simulate the moments of the position operators as functions of time in two separate ways: by simulating the Lindblad master equation on the one hand, and by first finding differential equations for the moments and solving those on the other hand. We will compare the results of these two approaches to see if they match up.

The conclusion is that the simple approach, where we find differential equations for the moments and solve those, gives better results than the full simulation of the Lindblad master equation. This is a consequence of the cutoff at finitely many levels of the QHOs, which likely results in coefficients which do not guarantee the positivity of the density matrix. There are general constraints on those coefficients, according to [5]; apparently, those conditions were not satisfied for this simulation. Furthermore, we conclude from these simulations that the noiseless clusters for $N = 3$ are preserved when adding the dissipation of a heat bath.

2 Noiseless Clusters

The theory of this paper is based on the application of the theory of open quantum systems to networks. We will first investigate networks in a setting where do not yet explicitly consider the heat bath; this we will do in section 3. Specifically, we will be looking at Erdös-Rényi graphs, which are a type of random graph with N nodes which are connected with a probability of p. Examples of such networks can be seen in the next section. In those networks we will apply the following Hamiltonian which can also be found in [6]:

$$\hat{\mathcal{H}} = \frac{1}{2}\sum_{i=1}^{N}\left(\hat{p}_i^2 + (\omega_i^2 + 2k_m)\hat{q}_i^2\right) - \sum_{i=1}^{N}\sum_{j=1}^{N}\lambda_{ij}(1-\delta_{ij})\hat{q}_i\hat{q}_j \tag{2.1}$$

This Hamiltonian is a sum of N harmonic oscillators and an interaction term. Here we have $\hat{p}_i$ and $\hat{q}_i$ represent the momentum and position operators of node i of the graph; ω_i is the normal frequency of each individual node. The λ_{ij} are the elements of the adjacency matrix of the graph, and the δ_{ij} is just the Kronecker delta. Finally, the k_m is a constant which is chosen in such a way that the whole Hamiltonian becomes positive-definite. A sufficient condition for this choice of k_m is slightly larger than the maximum sum of couplings of any node (that is, $\max_i\left(\sum_j \lambda_{ij}\right)$); this results from the strict diagonal dominance criterion for positive definiteness. So, the Hamiltonian consists of a diagonal term and the adjacency matrix.

We will assume that all the nodes are coupled in the same way to the same bath, from which we can and will later derive that the bath acts on the center of mass, $\hat{q}_{cm} = \sum_{n=1}^{N}\hat{q}_n$. This means that if we find an eigenvector $v = (v_1, \dots v_n)$ of the Hamiltonian which are orthogonal to $\hat{q}_{cm}$, that is, $\sum_{n=1}^{N} v_n = 0$, then we have found a noiseless cluster.

2.1 The case $N = 3$

How do we find such noiseless clusters? By diagonalizing the Hamiltonian. We will often make this assumption, that $\omega_i = \omega, \forall i \in \{1, \dots, N\}$, since if every node has the same base frequency, we only need to diagonalize the adjacency matrix, as the other terms are already diagonal. It might be enlightening to look at this hamiltonian in its quadratic form:

$$\hat{\mathcal{H}} = \frac{1}{2}\left(p^T p + q^T\left(\omega^2 + 2k_m\right)q\right) + q^T\Lambda q$$

Here, Λ is the adjacency matrix, containing the λ_{ij}. We will look at a small example to see how we can find noiseless clusters, in the case where $N = 3$. In that case we have two options: a straight line or chain which we will call m_2, and a triangle which we will call m_3. A graphical depiction is shown in figure 1.

The adjacency matrices are:

$$\Lambda_2 = \begin{pmatrix} 0 & 1 & 0 \\ 1 & 0 & 1 \\ 0 & 1 & 0 \end{pmatrix}, \Lambda_3 = \begin{pmatrix} 0 & 1 & 1 \\ 1 & 0 & 1 \\ 1 & 1 & 0 \end{pmatrix}$$

Figure 1: *Graphical depiction of* m_2 ***(a)*** *and* m_3 ***(b)***

The diagonalization of these matrices can be done by hand, and for m_2 results in the the eigenvectors $(1, 0, -1)$, $(1, -\sqrt{2}, 1)$ and $(1, \sqrt{2}, 1)$. In matrix form, they are (after normalizing the eigenvectors):

$$\mathcal{F}_{m_2} = \frac{1}{2}\begin{pmatrix} 1 & \sqrt{2} & 1 \\ \sqrt{2} & 0 & -\sqrt{2} \\ 1 & -\sqrt{2} & 1 \end{pmatrix}$$

Of these, only $\frac{\sqrt{2}}{2}(1, 0, -1)$ represents a noiseless subsystem, since only that one adds to 0.

On the other hand, Λ_3 is a special case of a very interesting type of adjacency matrices, namely the set of Laplacian matrices. Those are matrices whose rows (and in this case by symmetry of the adjacency matrix also whose columns) add up to the same number. This means that $\hat{q}_{cm}$ is an eigenvector of the matrix. This in turn leads to the conclusion that all other eigenvectors are perpendicular to the center of mass, so that there are automatically $N - 1$ noiseless subsystems.

It is now easy to see that Λ_3 is indeed a Laplacian matrix, and so there are 2 noiseless subsystems. In fact, they are $(1, -1, 0)$ and $(0, 1, -1)$ or any linear combination of these two.

2.2 More general cases

We want to get a better view of the proportion of noiseless clusters and its dependence on the network topology (N and p). To this end, a simulation was run to generate Erdos-Renyi networks and analyze them. An Erdos-Renyi network is a type of random graph with node count N, and a probability of connection p for each possible connection (for each set of two nodes). Thus for each N and p we create a statistical ensemble $\mathcal{G}(N, p)$. Such a network can be connected (that is, consisting of only one component) with a certain probability $P_{conn}(N, p)$, which is increasing in p, and steepest at $p_c = ln(N)/N$ [6]. In the simulation, the adjacency matrix was diagonalized and the noiseless clusters (if present) were counted for $N = 3, \ldots, 30$, and p attaining 75 equidistant points between 0 and 1. The result of this simulation is shown in figure 2. All images were created with the use of Matplotlib [7].

You will notice that this figure closely resembles the one in [6]. So what can be seen in this image? One thing that is apparent is the tendency for noiseless clusters

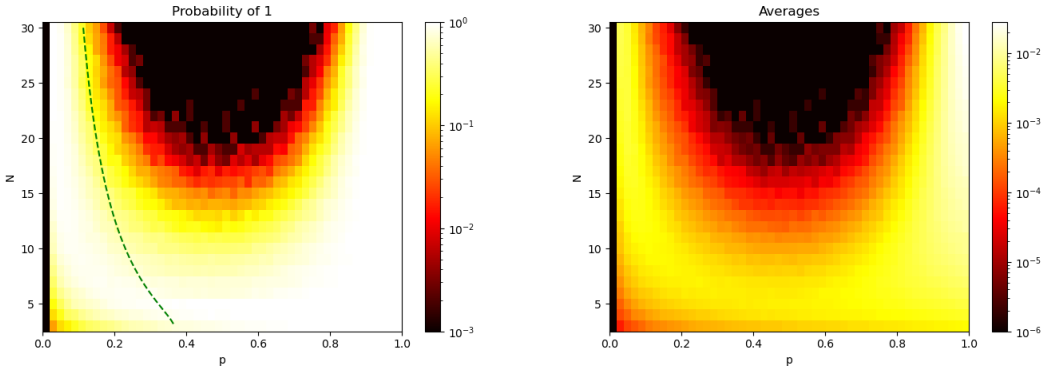

(a) ***(b)***

Figure 2: *The fraction of noiseless subsystems out of the total* ***(b)*** *and the probability to find at least one noiseless subsystem* ***(a)****, depending on the number of nodes in the network* N *and the probability of connection* p*. The green line in* ***(b)*** *corresponds to* $p_c = ln(N)/N$*, the line along which the slope of the function* P_{conn} *is steepest.*

to be located in either high or low probability regions. For low p, this results from a high probability of finding small clusters like the ones for $N = 3$ that we saw, and both of those had a noiseless subsystem.

3 The Lindblad master Equation

Up until now, we've considered the adjacency matrix and its eigenvectors to see if we can find eigenvectors that sum up to 0; the noiseless eigenvectors. But this is a rather simple view of the matter; we would like to go a bit more in-depth by considering how exactly the bath acts on the system. To do this, we need what is called the Lindblad master Equation. It looks like this:

$$\frac{d\rho(t)}{dt} = -i[H,\rho(t)] - \frac{1}{4}\sum_n i\Gamma_n([Q_n,\{P_n,\rho(t)\}] - [P_n,\{Q_n,\rho(t)\}]) \\ +D_n\left([Q_n,[Q_n,\rho(t)]] - \frac{1}{\Omega_n^2}[P_n,[P_n,\rho(t)]]\right) \tag{3.1}$$

We want to derive this equation; the meaning of all these symbols will become clear through the process of derivation. This derivation will follow [8] and [9]. To do so, we need to understand how open quantum systems work in general. Let us start from the ground up, beginning with the basics of quantum mechanics (a short review), an overview of density matrices, completely positive trace-preserving (CPT) maps, and finally the derivation of the Lindblad equation.

3.1 Basics

We're working in a Hilbert space, as always in quantum mechanics, and we denote it by $\mathcal{H}$. In this Hilbert space we have our kets: $|\psi\rangle \in \mathcal{H}$. Every ket has a bra, its dual vector: $\langle\psi|$. Together they form the scalar (inner) product: $\langle\psi|\phi\rangle \in \mathbb{C}$.

We have operators which can act on the kets, and we have a notation for the space of bounded operators: $B : \mathcal{H} \to \mathcal{H}$. We have a very special type of operator in this space, namely those formed by an outer product: $|\psi\rangle\langle\phi|$, with $(|\psi\rangle\langle\phi|)\varphi = \langle\phi|\varphi\rangle|\psi\rangle$. When it comes to operators, there are a few concepts that we care about:

- Hermitian conjugate: for an operator A, its Hermitian conjugate is $A^\dagger$ such that $\langle A^\dagger\phi|\psi\rangle = \langle\phi|A\psi\rangle$ for any $|\phi\rangle$ and $|\psi\rangle$.
- Unitary operators: an operator U is unitary if $UU^\dagger = U^\dagger U = \mathbb{1}$, the identity operator.
- Hermitian operators: an operator H is Hermitian if $H^\dagger = H$.
- Positivity: an operator P is positive, and we write $P > 0$ like one might expect, if $\forall\psi \in H$ we have $\langle\psi|P|\psi\rangle > 0$.
- Commutators and anti-commutators: in quantum mechanics, we often make use of the following two operations on operators, namely the commutator $[A,B] = AB - BA$ and the anti-commutator $\{A,B\} = AB + BA$. If A and B commute, these are equal to 0 and $2AB$, respectively.

- Trace: for an operator A, we can find its trace $\mathrm{Tr}[A]$ by looking at it in a certain basis and adding the diagonal elements of the matrix representation in that basis. The choice of basis doesn't matter; this we will see this next.

The last one we will look at and describe in a bit more detail, as we will need it plenty of times. The trace has the following properties:

- The cyclic property: for any two operators $P_1, P_2 \in \mathcal{H}$, the cyclic property says that $\mathrm{Tr}[P_1 P_2] = \mathrm{Tr}[P_2 P_1]$.
- Basis invariance: the trace is independent of the choice of basis with which we determine the matrix representation. This is pretty important to have a well-defined trace.

We will prove both of these statements:

Proof. In both cases, take a basis $|1\rangle, \ldots, |n\rangle$; let's denote the matrix representation of A and B by the same letters:

$$A = \begin{bmatrix} \mathbf{a_1} & \ldots & \mathbf{a_n} \end{bmatrix} = \begin{bmatrix} A_1 \\ \vdots \\ A_n \end{bmatrix}, B = \begin{bmatrix} \mathbf{b_1} & \ldots & \mathbf{b_n} \end{bmatrix} = \begin{bmatrix} B_1 \\ \vdots \\ B_n \end{bmatrix}$$

- We will actually calculate $\mathrm{Tr}\big[B^T A\big]$:

$$\begin{aligned} \mathrm{Tr}\big[B^T A\big] &= \sum_i \langle i|B^T A|i\rangle = \sum_i \mathbf{b_i}^T \mathbf{a_i} = \sum_{i,j} A_{ij} B_{ij} = \\ &= \sum_j A_j B_j^T = \sum_j \langle j|AB^T|j\rangle = \mathrm{Tr}\big[AB^T\big] \end{aligned}$$

  The second formulation follows quite trivially from the first.

- Let B be the change of basis operator, we can derive that $\mathrm{Tr}[BAB^{-1}] = \mathrm{Tr}[B^{-1}BA] = \mathrm{Tr}[A]$, so that indeed our choice of basis doesn't matter.

□

3.2 Density matrices

With this information refreshed, we will jump onwards to density matrices. A density matrix is used to describe mixed states; let us examine n states $|\psi_1\rangle, \ldots, |\psi_n\rangle$ which each occur with probability p_i respectively. Then we define the density matrix as follows:

$$\rho = \sum_i p_i |\psi_i\rangle\langle\psi_i| \tag{3.2}$$

The density matrix has two very interesting properties, which we will see more of later:

- Unit trace: $\mathrm{Tr}[\rho] = 1$. To see this, calculate the trace in the $|\psi\rangle_i$ basis: $\mathrm{Tr}[\rho] = \sum_j \langle\psi_j|\rho|\psi_j\rangle = \sum_i \sum_j p_i \langle\psi_j|\psi_i\rangle\langle\psi_i|\psi_j\rangle = \sum_i p_i = 1$ by orthonormality and because the probabilities must add to one.

- Hermitian: the density matrix is Hermitian; this follows from the fact that $(|\psi_i\rangle\langle\psi_i|)^\dagger = \langle\psi_i|^\dagger|\psi_i\rangle^\dagger = |\psi_i\rangle\langle\psi_i|$.

- Positivity: the density matrix is positive-semidefinite (and so the corresponding density operator is positive). This follows directly from the definition (equation 3.2); to see this, just multiply on the right by $|\psi_i\rangle$.

The density matrix can also be used to calculate the expectation values of operators. For a given operator A, the expectation value is given by

$$\langle A\rangle = \mathrm{Tr}[A\rho] \tag{3.3}$$

This we will not derive (although it isn't so difficult); instead, we will move forwards by seeing how the density matrix combines with the Schrodinger equation to get the Von Neumann equation. The Schrodinger equation is as follows:

$$i\hbar\frac{d}{dt}|\psi(t)\rangle = H|\psi(t)\rangle \tag{3.4}$$

From now on we will choose the units in such a way as to make $\hbar = 1$. We can then combine the two equations to find an expression for the derivative of ρ:

$$\begin{aligned}\dot{\rho} &= \sum_i p_i\left(\frac{d|\psi_i\rangle}{dt}\langle\psi_i| + |\psi_i\rangle\frac{d\langle\psi_i|}{dt}\right) = -i\sum_i p_i\big(H|\psi_i\rangle\langle\psi_i| - |\psi_i\rangle\langle\psi_i|H^\dagger\big)\\ &= -i(H\rho - \rho H) = -i[H,\rho]\end{aligned} \tag{3.5}$$

Where we used (amongst other things) the fact that H is Hermitian. This equation is called the Von Neumann equation. Now we want to apply this equation to a system with its environment. To achieve that we describe our full Hamiltonian in terms of tensor products. If we have N subsystems (N nodes) then the full Hamiltonian is given by

$$\mathcal{H} = \mathcal{H}_1 \otimes \mathcal{H}_1 \otimes \ldots \otimes \mathcal{H}_N$$

In a similar way, the full density matrix for N mixed states is given by $\rho = \rho_1 \otimes \ldots \otimes \rho_N$. We also define the partial trace. In the case of two nodes a and b with density matrices ρ_a and ρ_b:

$$\mathrm{Tr_b}[\rho_a \otimes \rho_b] = \rho_a \,\mathrm{Tr}\,\rho_b = \rho_a$$

In this way we can regain the density matrix of a single system from the combined density matrix of many systems. More generally, the partial trace is defined as

$$\mathrm{Tr_b}\left[\sum_{i,j,k,l} c_{ijkl}|a_i\rangle\langle a_j| \otimes |b_k\rangle\langle b_l|\right] \equiv \sum_{i,j}|a_i\rangle\langle a_j|\,\mathrm{Tr}\left[\sum_{k,l} c_{ijkl}|b_k\rangle\langle b_l|\right]$$

3.3 CPT-maps

We must define yet another concept: that of CPT-maps. This stands for Completely Positive, Trace-preserving Maps. This is because we want to know which types of maps will preserve the properties of a density matrix (unit trace, positivity, and Hermicity). Firstly, we should know what a positive map is:

Definition 3.1. A map $\mathcal{V}$ is positive if $\forall A \in B(\mathcal{H}) : A \geq 0 \implies \mathcal{V}A \geq 0$.

The properties of a CPT-map are then as follows:

- Trace-preserving: $\mathcal{V}$ is trace-preserving if $\mathrm{Tr}[\mathcal{V}A] = \mathrm{Tr}[A], \forall A \in O(\mathcal{H})$.
- Completely positive: $\mathcal{V}$ is completely positive if $\forall n \in \mathbb{N}$ the following holds: $\mathcal{V} \otimes \mathbb{1}_n$ is positive.

The definition for completely positive and positive are not the same, see [8]. We need complete positivity because there might be subsystems whose density matrix should still be positive.

3.4 Microscopic Derivation

Now we want to apply our acquired knowledge to the system of which we want to know the Lindblad master Equation. We will describe our system with this Hamiltonian:

$$H_T = H \otimes \mathbb{1}_E + \mathbb{1}_S \otimes H_E + H_I = H \otimes \mathbb{1}_E + \mathbb{1}_S \otimes H_E + \sum_i S_i \otimes E_i \tag{3.6}$$

We will look at the system in the so-called "interaction picture". This means that every operator O has a corresponding time-dependent operator $\hat{O}(t)$, given by $\hat{O}(t) = e^{i(H+H_E)t} O e^{-i(H+H_E)t}$. Notice that $H + H_E$ commutes with $e^{-i(H+H_E)t}$, so that $H + H_E$ does not change in the interaction picture. After this switch, the time evolution of the density matrix is given by

$$\frac{d\hat{\rho}_T(t)}{dt} = -i\Big[\hat{H}_I(t), \hat{\rho}_T(t)\Big] \tag{3.7}$$

Integrating this results in the following equation:

$$\hat{\rho}_T(t) = \hat{\rho}_T(0) - i\int_0^t \Big[\hat{H}_I(s), \hat{\rho}_T(s)\Big] ds \tag{3.8}$$

The annoying this about this is that $\hat{\rho}_T(t)$ still depends on previous values of $\hat{\rho}_T$. If we now fill in 3.8 into 3.7, we get the following:

$$\frac{d\hat{\rho}_T(t)}{dt} = -i\Big[\hat{H}_I(t), \hat{\rho}_T(0)\Big] - \int_0^t \Big[\hat{H}_I(t), \Big[\hat{H}_I(s), \hat{\rho}_T(s)\Big]\Big] ds$$

The full density matrix is still present in this equation, but we're only interested in the density matrix of the system itself, $\hat{\rho}$. So we use the partial trace like we introduced it earlier:

$$\frac{d\hat{\rho}(t)}{dt} = \mathrm{Tr}_E\left[\frac{d\hat{\rho}_T(t)}{dt}\right] = -i\,\mathrm{Tr}_E\Big[\hat{H}_I(t), \hat{\rho}_T(0)\Big] - \int_0^t \mathrm{Tr}_E\Big[\hat{H}_I(t), \Big[\hat{H}_I(s), \hat{\rho}_T(s)\Big]\Big] ds \tag{3.9}$$

We will now make a few more assumptions: we choose $\rho_T(0) = \rho(0) \otimes \rho_E(0)$; that is, the system and its environment are initially uncorrelated. Furthermore, we assume a particular shape for the density matrix of the environment: $\hat{\rho}_E(0) = e^{-\hat{H}_E\beta}$. $\mathrm{Tr}\Big[e^{-\hat{H}_E\beta}\Big]^{-1}$, where $\beta = 1/k_BT$. This immediately implies that $\Big[\hat{H}_E, \hat{\rho}_E(0)\Big] = 0$, this will be of use to us later. Now we can simplify the first term of the right hand side of 3.9:

$$\mathrm{Tr}_E\Big[\hat{H}_I(t), \hat{\rho}_T(0)\Big] = \sum_i \Big(\hat{S}_i(t)\hat{\rho}(0)\,\mathrm{Tr}_E\Big[\hat{E}_i(t)\hat{\rho}_E(0)\Big] - \hat{\rho}(0)\hat{S}_i(t)\,\mathrm{Tr}_E\Big[\hat{\rho}_E(0)\hat{E}_i(t)\Big]\Big) \tag{3.10}$$

Here we make yet another assumption: that $\langle E_i\rangle = \mathrm{Tr}[E_i\rho_E(0)] = 0$. This assumption is justified; if it isn't true, then we can slightly adjust the full hamiltonian: $H_T = (H + \sum_i \langle E_i\rangle S_i) + H_E + H_i'$, where $H_i' = \sum_i S_i \otimes (E_i - \langle E_i\rangle)$. So, we have now set the expectation value of the interaction Hamiltonian to zero without changing the dynamics of the system; we have only added a constant to it. Due to the cyclic property of the trace ($\mathrm{Tr}[AB] = \mathrm{Tr}[BA]$), all of equation 3.10 is equal to 0. So we are left with:

$$\frac{d\hat{\rho}(t)}{dt} = -\int_0^t \mathrm{Tr}_E\Big[\hat{H}_I(t), \Big[\hat{H}_I(s), \hat{\rho}_T(s)\Big]\Big] ds \tag{3.11}$$

Here we still see the full density matrix $\hat{\rho}_T$; we want to work towards an expression with only $\hat{\rho}$. So we must make a stronger assumption: that the system is *always* uncorrelated with its environment, i.e. $\hat{\rho}_T(t) = \hat{\rho}(t) \otimes \hat{\rho}_E(0)$. This is called the Born approximation, and it results in:

$$\frac{d\hat{\rho}(t)}{dt} = -\int_0^t \mathrm{Tr}_E\Big[\hat{H}_I(t), \Big[\hat{H}_I(s), \hat{\rho}(s) \otimes \hat{\rho}_E(0)\Big]\Big] ds \tag{3.12}$$

Alas, we are not yet done. We want to make the equation Markovian; this means that we don't want the expression on the right to contain any information about the time or about previous values of $\hat{\rho}$. In this case, the expression still contains the time t, which means that it is not Markovian. To ensure that it becomes Markovian, we first replace $\hat{\rho}(s)$ by $\hat{\rho}(t)$ and we change the variable of integration: $s \to t - s$. The boundaries of integration do not change as a result of this. So we can now interpret s as a measure of how far we should look back in time to account for memory effects [10]. Now we apply the Markov-approximation: we assume that we can use ∞ as the upper bound of integration; this is equivalent to assuming that the memory effects amount to 0 in the full integral. Then we get the following:

$$\frac{d\hat{\rho}(t)}{dt} = -\int_0^\infty \mathrm{Tr}_E\Big[\hat{H}_I(t), \Big[\hat{H}_I(t-s), \hat{\rho}(t) \otimes \hat{\rho}_E(0)\Big]\Big] ds \tag{3.13}$$

This is known as the Redfield equation. Of course, we still have a number of steps to go, as this equation does not guarantee positivity of the density matrix. So we must apply what's called the rotating wave approximation. First we do need to write the equation in another basis, namely the basis of eigenvectors of the superoperator $\tilde{H}A \equiv [H, A]$. Thus we write

$$S_i = \sum_\omega S_i(\omega) \tag{3.14}$$

Where the following holds for $S_i(\omega)$:

$$[H, S_i(\omega)] = -\omega S_i(\omega) \tag{3.15}$$

The adjoint of such an operator is also an eigenvalue of the same superoperator:

$$\Big[H, S_i^\dagger(\omega)\Big] = -\Big[S_i^\dagger(\omega), H^\dagger\Big] = -[H, S_i(\omega)]^\dagger = \omega S_i^\dagger(\omega) \tag{3.16}$$

We now want to go back from the interaction picture to the Schrodinger picture. To that end, we take a look at $\tilde{S}_k = e^{itH} S_k e^{-itH}$. We will first rewrite this with the use of equation 3.15. We look at $S_k H^n$:

$$\begin{aligned} S_k H^n &= (S_k H) H^{n-1} = (S_k H - H S_k + H S_k) H^{n-1} = ([S_k, H] + H S_k) H^{n-1} \\ &= (\omega S_k + H S_k) H^{n-1} = (\omega I + H)\big(S_k H^{n-1}\big) = \ldots = \\ &= (\omega I + H)^n S_k \end{aligned}$$

Now we can find a nice expression for $\tilde{S}_k$, and therefore also for $\tilde{H}_I(t)$:

$$\begin{aligned} \tilde{H}_I(t) &= \sum_k \tilde{S}_k(t) \otimes \tilde{E}_k(t) = \sum_{k,\omega} \big(e^{itH} S_k e^{-itH}\big) \otimes \tilde{E}_k(t) \\ &= \sum_{k,\omega} \left(e^{itH} \sum_{n=0}^{\infty} \frac{(-it)^n}{n!} S_k H^n \right) \otimes \tilde{E}_k(t) \\ &= \sum_{k,\omega} \left(e^{itH} \sum_{n=0}^{\infty} \frac{(-it)^n}{n!} (\omega I + H)^n S_k \right) \otimes \tilde{E}_k(t) \\ &= \sum_{k,\omega} \big(e^{itH} e^{-itH} e^{-it\omega} S_k\big) \otimes \tilde{E}_k(t) = \sum_{k,\omega} e^{-it\omega} S_k(\omega) \otimes \tilde{E}_k(t) \end{aligned} \tag{3.17}$$

In a similar way we find:

$$\tilde{H}_I(t) = \sum_{k,\omega} e^{it\omega} S_k^\dagger(\omega) \otimes \tilde{E}_k^\dagger(t) \tag{3.18}$$

We now expand all the commutators of the Redfield equation (3.13):

$$\dot{\hat{\rho}}(t) = -\operatorname{Tr}_E\Big[\int_0^\infty \hat{H}_I(t)\hat{H}_I(t-s)\hat{\rho}(t)\otimes\hat{\rho}_E(0)ds - \int_0^\infty \hat{H}_I(t)\hat{\rho}(t)\otimes\hat{\rho}_E(0)\hat{H}_I(t-s) - \int_0^\infty \hat{H}_I(t-s)\hat{\rho}(t)\otimes\hat{\rho}_E(0)\hat{H}_I(t)ds + \int_0^\infty \hat{\rho}(t)\otimes\hat{\rho}_E(0)\hat{H}_I(t-s)\hat{H}_I(t)\Big] \tag{3.19}$$

Filling in 3.17 and 3.18 into 3.19 is quite a lot of work; we will only look at the first term. Note that we fill in the first representation (3.17) whenever we encounter an $\tilde{H}(t-s)$, and we the second representation (3.18) for $\tilde{H}(t)$:

$$\begin{aligned}
&\operatorname{Tr}_E\Big[\int_0^\infty \tilde{H}_I(t)\tilde{H}_I(t-s)\hat{\rho}(t)\otimes\hat{\rho}_E(0)\Big] \\
&= \operatorname{Tr}_E\Big[\int_0^\infty \Big(\sum_{\omega',k} e^{i\omega' t}S_k^\dagger(\omega')\otimes\tilde{E}_k^\dagger(t)\Big)\Big(\sum_{\omega,l} e^{-i\omega(t-s)}S_l(\omega)\otimes\tilde{E}_l(t-s)\Big)(\hat{\rho}(t)\otimes\hat{\rho}_E(0))ds\Big] \\
&= \operatorname{Tr}_E\Big[\int_0^\infty \sum_{\omega,\omega',k,l} e^{i(\omega'-\omega)t}e^{i\omega s}\Big(S_k^\dagger(\omega')S_l(\omega)\hat{\rho}(t)\Big)\otimes\Big(\tilde{E}_k^\dagger(t)\tilde{E}_l(t-s)\hat{\rho}_E(0)\Big)ds\Big] \\
&= \sum_{\omega,\omega',k,l} e^{i(\omega'-\omega)t}S_k^\dagger(\omega')S_l(\omega)\hat{\rho}(t)\cdot\operatorname{Tr}\int_0^\infty e^{i\omega s}\tilde{E}_k^\dagger(t)\tilde{E}_l(t-s)\hat{\rho}_e(0)ds \\
&= \sum_{\omega,\omega',k,l} e^{i(\omega'-\omega)t}\Gamma_{kl}(\omega)S_k^\dagger(\omega')S_l(\omega)\hat{\rho}(t)
\end{aligned}$$

Where we have defined:

$$\Gamma_{kl}(\omega) \equiv \int_0^\infty e^{i\omega s}\operatorname{Tr}\Big[\tilde{E}_k^\dagger(t)\tilde{E}_l(t-s)\hat{\rho}_e(0)\Big]ds \tag{3.20}$$

In a similar way we work out the other terms to come to:

$$\dot{\hat{\rho}}(t) = \sum_{\substack{\omega,\omega'\\k,l}}\Big(e^{i(\omega'-\omega)t}\Gamma_{kl}(\omega)\Big[S_l(\omega)\hat{\rho}(t),S_k^\dagger(\omega')\Big] + e^{i(\omega-\omega')t}\Gamma_{lk}^*(\omega')\Big[S_l(\omega),\hat{\rho}(t)S_k^\dagger(\omega')\Big]\Big) \tag{3.21}$$

Now we can finally apply the rotating wave approximation: we assume that all the terms with $\omega' \neq \omega$ contribute insignificantly to the sum, seen as they oscillate much faster than the typical timescales of the system. The equation then becomes as follows:

$$\dot{\hat{\rho}}(t) = \sum_{\substack{\omega,\omega\\k,l}}\Big(\Gamma_{kl}(\omega)\Big[S_l(\omega)\hat{\rho}(t),S_k^\dagger(\omega)\Big] + \Gamma_{lk}^*(\omega)\Big[S_l(\omega),\hat{\rho}(t)S_k^\dagger(\omega)\Big]\Big) \tag{3.22}$$

This was the last approximation; from now on we only need to rewrite it before we can call it the Lindblad equation. First we separate the hermitian and non-hermitian parts of Γ_{kl}:

$$\Gamma_{kl}(\omega) = \frac{1}{2}\gamma_{kl}(\omega) + i\pi_{kl}(\omega)$$
$$2i\pi_{kl}(\omega) \equiv \Gamma_{kl}(\omega) - \Gamma^*_{lk}(\omega)$$
$$\gamma_{kl}(\omega) \equiv \Gamma_{kl}(\omega) + \Gamma^*_{lk}(\omega)$$

If we fill these in, we arrive quite readily to this equation:

$$\dot{\hat{\rho}}(t) = -i[H_{Ls}, \hat{\rho}(t)] + \sum_{\omega,k,l} \gamma_{kl}(\omega)\left(S_l(\omega)\hat{\rho}(t)S_k^\dagger(\omega) - \frac{1}{2}\Big\{ S_k^\dagger(\omega)S_l(\omega), \hat{\rho}(t) \Big\}\right)$$

Where $H_{Ls} = \sum_{\omega,k,l} \pi_{kl}(\omega)S_k^\dagger(\omega)S_l(\omega)$. This extra Hamiltonian is called the "Lamb shift" Hamiltonian. If we now transform back to the Schrodinger picture, we only receive an extra H in the commutator:

$$\dot{\rho}(t) = -i[H + H_{Ls}, \rho(t)] + \sum_{\omega,k,l} \gamma_{kl}(\omega)\left(S_l(\omega)\rho(t)S_k^\dagger(\omega) - \frac{1}{2}\Big\{ S_k^\dagger(\omega)S_l(\omega), \rho(t) \Big\}\right) \tag{3.23}$$

This equation also has a name: the Markovian master equation. This is not yet the final result; it is not yet in Lindblad form. We now want to remove the non-diagonal terms ($S_l\rho S_k$ with $l \neq k$) from the equation. And this is possible: the coefficients γ_{kl} form a positive matrix by Bochner's theorem [11], so it can be diagonalized.

This step will be explained in more detail in section 3.5, where we'll also apply the equation to the specifics of our situation, the Erdos-Renyi networks. The equation we now get, the Lindblad master equation, is as follows:

$$\dot{\rho}(t) = -i[H + H_{Ls}, \rho(t)] + \sum_{\omega,i} \left(L_i(\omega)\rho(t)L_i^\dagger(\omega) - \frac{1}{2}\Big\{ L_i^\dagger(\omega)L_i(\omega), \rho(t) \Big\}\right) \equiv \mathcal{L}\rho(t) \tag{3.24}$$

In many cases [8] there is only one relevant frequency, and then we can perform one more step to simplify the equation:

$$\dot{\rho}(t) = -i[H + H_{Ls}, \rho(t)] + \sum_{i} \left(L_i\rho(t)L_i^\dagger - \frac{1}{2}\Big\{ L_i^\dagger L_i, \rho(t) \Big\}\right) \equiv \mathcal{L}\rho(t) \tag{3.25}$$

The L_i's in this equation are called the "Lindblad operators".

3.5 Application

Now we have seen the Lindblad equation in its full generality; however, we still don't know how to apply it yet to our situation. We wish to find the jump operators for our networks, and in order to get there we will redo some of the steps of the derivation

that we just saw. We begin by formulating the Hamiltonians of our system, of the bath, and their interaction, using the same definitions as in [6]. For the system Hamiltonian we have

$$\hat{\mathcal{H}} = \frac{1}{2}\sum_{i=1}^{N}\left(\hat{p}_i^2 + (\omega_i^2 + 2k_m)\hat{q}_i^2\right) - \sum_{i=1}^{N}\sum_{j=1}^{N}\lambda_{ij}(1-\delta_{ij})\hat{q}_i\hat{q}_j \tag{3.26}$$

Here λ_{ij} is an element of the adjacency matrix.

For the bath Hamiltonian, (aka the environment Hamiltonian) we take an infinite collection of harmonic oscillators:

$$\hat{\mathcal{H}}_E = \frac{1}{2}\sum_{a=1}^{\infty}\left(\frac{\hat{K}_\alpha^2}{M_\alpha} + \nu_\alpha^2\hat{X}_\alpha^2\right) \tag{3.27}$$

And finally, the interaction Hamiltonian:

$$\hat{\mathcal{H}}_I = -\sqrt{\gamma}\cdot\hat{q}_{cm}\otimes\hat{B} = -\sqrt{\gamma}\sum_{n=1}^{N}\hat{q}_n\otimes\sum_{a=1}^{\infty}\lambda_a\hat{X}_a \tag{3.28}$$

We will rewrite this in terms of the normal modes of the adjacency matrix. The normal modes are contained in the rotation matrix $\mathcal{F}$ [6], and originate from the diagonalization of the adjacency matrix:

$$\hat{\mathcal{H}} = \frac{1}{2}\left(P^TP + Q^T\mathcal{D}Q\right) = \frac{1}{2}\left(p^Tp + q^T\mathcal{M}q\right) \tag{3.29}$$

Where $\mathcal{M}$ is the matrix with all the couplings between the various coordinates, like in equation 2.1. Also, P, Q, p, and q are vectors containing all the position and momentum operators in the mode and node basis, respectively. So it must hold that $\mathcal{D} = \mathcal{F}^T\mathcal{M}\mathcal{F}$. It is clear now that $\mathcal{D}$ is a diagonal matrix, and we call its elements Ω_n^2. So now we write: $Q = \mathcal{F}^Tq$, that is $q = \mathcal{F}Q$. So we get:

$$\hat{\mathcal{H}}_I = -\sqrt{\gamma}\sum_{n=1}^{N}\kappa_n\hat{Q}_n\otimes\hat{B} = \sum_{n=1}^{N}S_i\otimes E_i \tag{3.30}$$

Here we have defined that $\kappa_n = \sum_{m=1}^{N}\mathcal{F}_{mn}$, and $S_i = -\sqrt{\gamma}\kappa_n\hat{Q}_n$. Now we have created the same form as in 3.6. We define the constants $\Gamma_n = \kappa_n^2\gamma$ and $D_n = \kappa_n^2\gamma\Omega_n\coth(\Omega_n/2T)$, where we chose units such that $k_B = 1$. If we plug all this information into the general form of the Lindblad master equation, we will arrive at the Lindblad master equation for our networks:

$$\begin{aligned}\frac{d\rho(t)}{dt} = -i[H,\rho(t)] - \frac{1}{4}\sum_n i\Gamma_n([Q_n,\{P_n,\rho(t)\}] - [P_n,\{Q_n,\rho(t)\}]) \\ +D_n\left([Q_n,[Q_n,\rho(t)]] - \frac{1}{\Omega_n^2}[P_n,[P_n,\rho(t)]]\right)\end{aligned}$$

This, however, we will not derive.

4 Methods

Now that we have fully derived the Lindblad master equation, we want to connect it to the simpler situation in section 2 to check if that was justified. From the Lindblad master equation, we can calculate the moments of the position and momentum operators in the mode basis. In theory, this can be done in two ways: by directly calculating ρ from equation 3.1, or by first tracing that equation to find a different set of differential equations for both the first order: $\langle Q_n \rangle$ and $\langle P_n \rangle$, and for the second order: $\langle Q_n Q_m \rangle$, $\langle P_n P_m \rangle$ and $\langle \{Q_n, P_m\} \rangle$. We can solve those differential equations — to some degree analytically, and numerically otherwise — and thus find the moments of the position operators, which we are most interested in. We will begin by looking at the direct simulation, and then consider the set of differential equations for the moments, followed by their analytic solutions.

4.1 Density matrix

For the direct simulation, we need to consider what the shape of the superoperator $\tilde{\mathcal{L}}$ is for the density matrix in the normal mode basis, that is, the basis of eigenvectors of the Hamiltonian. The first term can be found most easily, as it only contains a commutator with the Hamiltonian. Now we must really solve the Schrodinger equation in order to find the eigenstates of the Hamiltonian.

We use the typical approach with the quantum ladder operators. We won't show the details of the derivation, but instead assume that the reader knows a little bit about quantum harmonic oscillators. We define

$$A_i = \sqrt{\frac{\Omega_i}{2}} Q_i + i \frac{P_i}{\sqrt{2\Omega_i}} \tag{4.1}$$

Now we can see that the Hamiltonian can be written as

$$H = \sum_{i=1}^{N} \Omega_i \left(A_i^\dagger A_i + \frac{1}{2} \right) = \sum_{i=1}^{N} \Omega_i \left(N_i + \frac{1}{2} \right) \tag{4.2}$$

Where $N_i = A_i^\dagger A_i$, and, like one might expect: $N_i |n\rangle_i = n |n\rangle_i$. So now we know the energy eigenvalues. :

$$H|n_1 n_2 \dots n_N\rangle = E_{n_1,n_2,\dots,n_N} |n_1 n_2 \dots n_N\rangle = \sum_{i=1}^{N} \Omega_i \left(n_i + \frac{1}{2} \right) |n_1 n_2 \dots n_N\rangle \tag{4.3}$$

We see that the Hamiltonian is now diagonal, which is good, because that's what usually happens when you successfully diagonalize an operator.

From now on, to keep the notation a bit more concise, we will abbreviate $(n_1, n_2, \dots, n_N) \equiv \mathbf{n}$, with $\mathbf{n} \in \mathbb{N}_0^N \equiv \mathcal{N}$, where $\mathbb{N}_0$ includes 0. In that notation, we have $H|\mathbf{n}\rangle = \mathbf{\Omega}^T (\mathbf{n} + \frac{1}{2}) |\mathbf{n}\rangle \equiv E_{\mathbf{n}} |\mathbf{n}\rangle$. We now want to calculate the first term of the Lindblad equation:

$$-i[H,\rho] = -i\sum_{\mathbf{n},\mathbf{m}\in\mathcal{N}} \rho_{\mathbf{nm}}[H,|\mathbf{n}\rangle\langle\mathbf{m}|] = -i\sum_{\mathbf{n},\mathbf{m}\in\mathcal{N}} \rho_{\mathbf{nm}}|\mathbf{n}\rangle\langle\mathbf{m}|(E_{\mathbf{n}} - E_{\mathbf{m}}) \tag{4.4}$$

Now we bravely soldier on to find the superoperator $\tilde{\mathcal{L}}$. In the next few terms of the Lindblad master equation, we see position and momentum operators. We must express these in terms of the ladder operators:

$$Q_n = \frac{1}{\sqrt{2\Omega_n}}\left(A_n + A_n^\dagger\right) \tag{4.5}$$

$$P_n = -i\sqrt{\frac{\Omega_n}{2}}\left(A_n - A_n^\dagger\right) \tag{4.6}$$

Let's find the matrix representation of the ladder operators in the basis of Hamiltonian eigenstates. For a single node, it is as follows:

$$A^\dagger = \begin{pmatrix} 0 & 0 & \cdots & 0 & \cdots \\ \sqrt{1} & 0 & \cdots & 0 & \cdots \\ 0 & \sqrt{2} & \ldots & 0 & \cdots \\ \vdots & \vdots & \ddots & \vdots & \cdots \\ 0 & 0 & \cdots & \sqrt{n} & \cdots \\ \vdots & \vdots & \vdots & \vdots & \ddots \end{pmatrix}, A = \begin{pmatrix} 0 & \sqrt{1} & 0 & \cdots & 0 & \cdots \\ 0 & 0 & \sqrt{2} & \ldots & 0 & \ldots \\ \vdots & \vdots & \vdots & \ddots & \vdots & \ldots \\ 0 & 0 & 0 & \ldots & \sqrt{n} & \ldots \\ \vdots & \vdots & \vdots & \vdots & \vdots & \ddots \end{pmatrix}$$

And Q and P are defined as in 4.5 and 4.6. For multiple nodes, we simply realize that A_i only acts on node i and leaves all other nodes unchanged; in mathematical terms this amounts to a tensor product with several identity matrices. If we let $\mathbb{1}_\infty$ be equal to a matrix of size $\mathbb{N}\times\mathbb{N}$ with 1s on the diagonal (like a countably infinite-dimensional identity matrix), then for N nodes, an operator A_i (where we can fill in either Q or P for A) is defined as:

$$A_i = \mathbb{1}_\infty^{\otimes n} \otimes A \otimes \mathbb{1}_\infty^{\otimes(N-n-1)}, n \in \{0,\ldots,N-1\}$$

You may have noticed that our matrices contain considerably more numbers than we would like to if we wish to actually implement it in a computer (specifically, infinitely many more), so at some point we must decide a maximal state to consider. In fact, let's do that now. We choose a maximal state number s, so that we have N nodes, s states that any one node can occupy, s^N basis vectors of our Hamiltonian, and so $\left(s^N\right)^2 = s^{2N}$ elements of the density matrix; so, we now use $\mathbb{1}_s$ instead of $\mathbb{1}_\infty$, and we cut off our P and Q matrices to be $s\times s$ matrices.

There is, however, one problem that arises when we cut off these states. Let's take a look at the position and momentum operators for example, and in particular, we want to calculate the commutator $[Q,P]$. From our knowledge of quantum mechanics, we expect to find $[Q,P] = i\mathbb{1}_s$. But this is not the case:

$$[Q,P] = i\begin{pmatrix} 1 & 0 & 0 & \dots & 0 \\ 0 & 1 & 0 & \dots & 0 \\ 0 & 0 & 1 & \dots & 0 \\ \vdots & \vdots & \vdots & \ddots & \vdots \\ 0 & 0 & 0 & \dots & 1-s \end{pmatrix} \tag{4.7}$$

So we see that this matrix looks very much like we'd expect, aside from the very last component, which actually decreases linearly with s. This is a problem; it means that as we try to simulate the density matrix with greater and greater accuracy, we're actually decreasing the accuracy because of the decreasing last component of the commutator. As far as could be discovered within the scope of this project, there is no easy fix for this problem that allows the simulation of the full Lindblad master equation; however, we can make an assumption which is justified in certain cases, namely that $D_n = 0$ for each n. We will see in section 4.2.1 that this simplification is justified as long as we only look at the first order moments of the position and momentum operators. This simplification allows the simulation to stay stable for about a dozen seconds. After that, the fastest decaying modes will quickly become unstable.

The parameters that we can vary to improve the duration in which the simulation is accurate are the time step dt and the maximal state number s. As it turns out, choosing a high s causes the graph to be more accurate for low t, but less accurate for high t; this can be compensated by choosing a very narrow dt. A rule of thumb that was used in the simulations of this project was to choose dt such that the first iteration preserves the properties of a density matrix (positive-semidefiniteness, Hermicity, and unit trace); of course, a certain tolerance for error is required to account for floating point errors. The specifics of the implementation can be found in section A of the appendix.

We are not yet ready to simulate the density matrix; we need to have some initial conditions as well. Calculating these is not super straightforward, seen as we want our initial condition to be a valid density matrix; that is, it must have unit trace and be Hermitian and positive. If we want our initial condition to have a nonzero expectation value for, let's say, all the Q_i operators, then we must first figure out what it looks like for one node. The claim is that an operator of a similar shape as the position operators themselves suffices for this purpose. What's also nice is that the Hermitian requirement is instantly fulfilled. Specifically, we define:

$$\rho_{Q_0^1} = \frac{1}{2\Omega_0}\begin{pmatrix} 0 & 1 & 0 & \dots & 0 & 0 \\ 1 & 0 & 1 & \dots & 0 & 0 \\ 0 & 1 & 0 & \dots & 0 & 0 \\ \vdots & \vdots & \vdots & \ddots & \vdots & \vdots \\ 0 & 0 & 0 & \dots & 0 & 1 \\ 0 & 0 & 0 & \dots & 1 & 0 \end{pmatrix} \tag{4.8}$$

Where the notation $\rho_{Q_0^1}$ means: an $s \times s$-matrix (for s-levels), and for 1 node, such that Q_0 (that is, the first coordinate, since arrays begin at zero) has nonzero

eigenvalue. In general we define (note the use of $A^{\otimes k}$ as the k-th tensor power of A):

$$\rho_{Q_i^N} = \mathbb{1}_s^{\otimes i} \otimes \rho_{Q_0^1} \otimes \mathbb{1}_s^{\otimes(N-i-1)}, \qquad i \in \{0, \dots, N-1\} \tag{4.9}$$

And we will use $\sum_i \rho_{Q_i^N}$ in the construction of our initial condition. This is not yet positive, and it doesn't have unit trace, but we solve this by putting a 2 on the main diagonal, and then dividing by $2Ns$.

Now we are ready to simulate the density matrix. See section 5 for the results.

4.2 Moments

Now we will consider the equations for the moments rather than the full Lindblad equation. Like in [12], we only look at the first and second order moments of the operators Q_n and P_n; this will suffice for Gaussian states. We will derive these from 3.1 in the normal mode basis. One thing we will use very often is the following equality:

$$[AB, C] = ABC - CAB = ABC - ACB + ACB - CAB = A[B, C] + [A, C]B \tag{4.10}$$

And similarly,

$$[A, BC] = ABC - BCA = ABC - BAC + BAC - BCA = [A, B]C + B[A, C] \tag{4.11}$$

Let's also quickly make a list of a few "standard" commutation relations we will need:

- $[P_n, H] = -i\Omega_n^2 Q_n$
- $[Q_n, H] = iP_n$
- $[P_n, Q_n^2] = [P_n, Q_n]Q_n + Q_n[P_n, Q_n] = -2iQ_n$
- $[P_n^2, Q_n] = P_n[P_n, Q_n] + [P_n, Q_n]P_n = -2iP_n$

4.2.1 First order

So now let's start with $\frac{d}{dt}\langle Q_n \rangle$:

$$\begin{aligned}\frac{d}{dt}\langle Q_n \rangle &= \operatorname{Tr}[Q_n \dot{\rho}] = -i \operatorname{Tr}[Q_n[H, \rho]] - \\ &\frac{1}{4}\sum_m i \operatorname{Tr}[\Gamma_m Q_n([Q_m, \{P_m, \rho\}] - [P_m, \{Q_m, \rho\}])] + \\ &\operatorname{Tr}\left[D_m Q_n \left([Q_m, [Q_m, \rho]] - \frac{1}{\Omega^2}[P_m, [P_m, \rho]]\right)\right]\end{aligned} \tag{4.12}$$

We will now look at these terms separately and without any of the prefactors, going from the back to the front, and we will see that many terms drop out. First we consider $m = n$:

$$\begin{aligned}\mathrm{Tr}[Q_n[P_n,[P_n,\rho]]] =& \mathrm{Tr}[Q_nP_nP_n\rho - Q_nP_n\rho P_n - Q_nP_n\rho P_n + Q_n\rho P_nP_n]\\ =&\langle Q_nP_nP_n - P_nQ_nP_n - (P_nQ_nP_n - P_nP_nQ_n)\rangle\\ =&\langle [Q_n,P_n]P_n - P_n[Q_n,P_n]\rangle = \langle iP_n - P_ni\rangle = 0\end{aligned}$$

The term with only Q_n drops out trivially by the cyclic property of the trace, and so let's consider the middle line. We expand all the commutators, distribute the Q_n, implement the cyclic property to put the ρ at the end and go back to an expectation value to get:

$$\begin{aligned}&\langle Q_nQ_nP_n + P_nQ_nQ_n - Q_nQ_nP_n - P_nQ_nQ_n\rangle +\\ &\langle P_nQ_nQ_n + Q_nP_nQ_n - Q_nP_nQ_n - Q_nQ_nP_n\rangle\\ =&\left\langle \left[P_n, Q_n^2\right]\right\rangle = -2i\langle Q_n\rangle\end{aligned}$$

We see that with the appropriate prefactors this results in $-\frac{i}{4}\Gamma_n \cdot -2i\langle Q_n\rangle = -\frac{1}{2}\Gamma_n\langle Q_n\rangle$. Furthermore, since $m \neq n \implies [Q_n, Q_m] = [Q_n, P_m] = 0$, we see that everything for $m \neq n$ cancels to 0. Now we still have to look at the first term with the system Hamiltonian; the commutator of Q_n and H is known. So we derive:

$$-i\,\mathrm{Tr}[Q_n[H,\rho]] = -i\,\mathrm{Tr}[Q_nH\rho - HQ_n\rho] = i\langle [H,Q_n]\rangle = \langle P_n\rangle$$

So now we can finally write:

$$\frac{d}{dt}\langle Q_n\rangle = \langle P_n\rangle - \frac{1}{2}\Gamma_n\langle Q_n\rangle \tag{4.13}$$

The derivation for the moment of momentum is very similar. This time, the part with only momenta drops out trivially, so we look at the left term on the bottom row:

$$\begin{aligned}\mathrm{Tr}[P_n[Q_n,[Q_n,\rho]]] =& \mathrm{Tr}[P_nQ_nQ_n\rho - P_nQ_n\rho Q_n - P_nQ_n\rho Q_n + P_n\rho Q_nQ_n]\\ =&\langle P_nQ_nQ_n - Q_nP_nQ_n - (Q_nP_nQ_n - Q_nQ_nP_n)\rangle\\ =&\langle [P_n,Q_n]Q_n - Q_n[P_n,Q_n]\rangle = \langle -iQ_n + Q_ni\rangle = 0\end{aligned}$$

For the first two terms:

$$\begin{aligned}&\langle\, P_nQ_nP_n + P_nP_nQ_n - Q_nP_nP_n - P_nQ_nP_n -\\ &\quad P_nP_nQ_n - Q_nP_nP_n + P_nP_nQ_n + Q_nP_nP_n\rangle\\ =&\left\langle \left[P_n^2, Q\right]\right\rangle = -2i\langle P_n\rangle\end{aligned}$$

With the right prefactor, this becomes a $-\frac{1}{2}\Gamma_n\langle P_n\rangle$. From the Hamiltonian we get a $-\Omega_n^2\langle Q_n\rangle$, and the result of the derivation is as follows:

$$\frac{d}{dt}\langle P_n\rangle = -\Omega_n^2\langle Q_n\rangle - \frac{1}{2}\Gamma_n\langle P_n\rangle \tag{4.14}$$

4.2.2 Second order

We also want to know the second order moments, namely $\frac{d}{dt}\langle Q_n Q_m\rangle$, $\frac{d}{dt}\langle P_n P_m\rangle$ and $\frac{d}{dt}\langle\{Q_n, P_m\}\rangle$. Let's start with $Q_n Q_m$ and look at the Hamiltonian term:

$$\begin{aligned}
&-i\,\mathrm{Tr}[Q_n Q_m[H,\rho]] = -i\,\mathrm{Tr}[Q_n Q_m H\rho - Q_n Q_m \rho H] \\
&= -i\,\mathrm{Tr}[Q_n Q_m H\rho - H Q_n Q_m \rho] = -i\langle[Q_n Q_m, H]\rangle \\
&= -i\langle Q_n[Q_m, H] + [Q_n, H]Q_m\rangle = \langle Q_n P_m + P_n Q_m\rangle
\end{aligned}$$

The next two terms can be calculated fairly simply by realizing that all the n operators commute with all the m operators except in the case $m = n$, so aside from then, we can always move one of the two to the front. So we get a term for n and for m:

$$\begin{aligned}
&\sum_i \Gamma_i\langle Q_n Q_m[Q_i,\{P_i,\rho\}]\rangle = \langle Q_n Q_m\Gamma_n[Q_n,\{P_n,\rho\}] + Q_n Q_m\Gamma_m[Q_m,\{P_m,\rho\}]\rangle = \\
&-2i\langle\Gamma_n Q_n Q_m + \Gamma_m Q_n Q_m\rangle = -2i(\Gamma_n+\Gamma_m)\langle Q_n Q_m\rangle
\end{aligned}$$

With the appropriate prefactor of $-\frac{i}{4}$, this becomes $-\frac{\Gamma_n+\Gamma_m}{2}\langle Q_n Q_m\rangle$. When $n = m$, it turns out we get $-\Gamma_n\langle Q_n^2\rangle$, which is actually the same as the other expression. We move on to the last two terms. For $m \neq n$ we can use the same trick as last time, and everything drops out. For $m = n$ the Q_n term drops out because everything commutes, so we only have to look at the P_n term (and let's leave out the n indices since it's all the same and because we want to be ~~lazy~~ efficient):

$$\begin{aligned}
\mathrm{Tr}\big[Q^2[P,[P,\rho]]\big] &= \mathrm{Tr}\big[Q^2P^2 - Q^2P\rho P - (Q^2P\rho P - Q^2\rho P^2)\big] \\
&= \big\langle (Q^2P - PQ^2)P - P(Q^2P - PQ^2)\big\rangle \\
&= \big\langle\big[\big[Q^2,P\big],P\big]\big\rangle = 2i\langle[Q,P]\rangle = -2
\end{aligned}$$

With the right prefactor of $\frac{D_n}{4\Omega_n^2}$, it becomes $-\frac{D_n}{2\Omega_n^2}$. Since this term only appears for $m = n$, we add a δ_{nm}. Then the full final expression becomes

$$\frac{d}{dt}\langle Q_n Q_m\rangle = \langle Q_n P_m + P_n Q_m\rangle - \frac{\Gamma_n+\Gamma_m}{2}\langle Q_n Q_m\rangle - D_n\frac{\delta_{nm}}{2\Omega_n^2} \tag{4.15}$$

Now we want to take a look at $\frac{d}{dt}\langle P_n P_m\rangle$; it's a very similar derivation. In the first step, we can swap all the P_n for the Q_n. The only other thing that changes is the constant; instead of the $[Q_n, H] = iP_n$ we get $[P_n, H] = -i\Omega_n^2 Q_n$. So the Hamiltonian term is given by $-\langle\Omega_n^2 Q_n P_n + \Omega_m^2 P_n Q_m\rangle$.

For the second row, we have the same situation as last time; when $m \neq n$, we can always move one of the operators to the front, and for $m = n$ the expression turns out to be the same. So we get exactly the same as in 4.15 but with the Q_n's replaced by P_n: $-\frac{\Gamma_n+\Gamma_m}{2}\langle P_n P_m\rangle$.

For the last row, the situation is again very similar to the last derivation: for $n \neq m$ it's all zero (always has been), and for $n = m$ we get a constant term (this

time without the $\frac{1}{\Omega_n^2}$ and with the opposite sign). The full expression for the second order momentum moment is thus as follows:

$$\frac{d}{dt}\langle P_n P_m\rangle = -\left\langle \Omega_n^2 Q_n P_m + \Omega_m^2 P_n Q_m \right\rangle - \frac{\Gamma_n + \Gamma_m}{2}\langle P_n P_m\rangle + D_n \frac{\delta_{nm}}{2} \tag{4.16}$$

Now we go for the mixed second order moment $\frac{d}{dt}\langle\{Q_n, P_m\}\rangle$. For the Hamiltonian term, the same strategy as in the second order position case will work; we replace Q_m by P_m and get

$$-i\,\mathrm{Tr}[Q_n P_m [H,\rho]] = -i\langle Q_n [P_m, H] + [Q_n, H] P_m\rangle = \left\langle -\Omega_m^2 Q_m Q_n + P_n P_m \right\rangle$$

For the opposite case with $P_m Q_n$, we get the exact same thing, because Q_n, P_n always commute with Q_m, P_m respectively, both for $m = n$ and for $m \neq n$. So, in the final result, an extra two will be added in front.

For the second row we will again make use of the fact that for $m \neq n$ we can move one of the operators to the front. But now instead of $Q_n Q_m$ or $P_n P_m$ we will get $\{Q_n, P_m\}$, as one might expect. So we have another term $-\frac{\Gamma_n+\Gamma_m}{2}\langle\{Q_n, P_m\}\rangle$.

The final row of the final moment; for $n \neq m$, everything drops out by the same reasoning as we have used many times before. For $n = m$ we do have to be a bit more careful. If we investigate the Q_n term, we see that after adding $Q_n P_n$ in front of it, it quickly reduces to this form:

$$\left\langle Q_n [P_n, Q_n] Q_n - Q_n^2 [P_n, Q_n] \right\rangle = 0$$

Since $[P_n, Q_n]$ is a constant. The reverse order drops out in a similar way. Now for the P_m (and final!) term. In fact, we don't even need to think about this anymore, since it's the same as what we just did, except with the P_n's and Q_n's swapped. So we can finally write down the equation for the mixed second order moment:

$$\frac{d}{dt}\langle\{Q_n, P_m\}\rangle = 2\langle P_n, P_m\rangle - 2\Omega_m^2\langle Q_n Q_m\rangle - \frac{\Gamma_n + \Gamma_m}{2}\langle\{Q_n, P_m\}\rangle \tag{4.17}$$

Actually, we aren't quite finished; both equation 4.15 and 4.16 contain $Q_n P_m$ and $P_n Q_m$, and we would like to rewrite those to only contain $\{Q_n, P_m\}$ so that we end up with three equations that only depend on each other. For $n \neq m$ we can easily see that since $[Q_n, P_m] = 0$, $\{Q_n, P_m\} = 2Q_n P_m = 2P_m Q_n$. For $n = m$ we can see that we can also compress the swapped operators into one anti-commutator. The final set of second order moments becomes as follows:

$$\begin{aligned}
\frac{d}{dt}\langle Q_n Q_m\rangle =& \frac{1}{2}\langle\{Q_n, P_m\} + \{P_n, Q_m\}\rangle \\
&- \frac{\Gamma_n + \Gamma_m}{2}\langle Q_n Q_m\rangle - D_n\frac{\delta_{nm}}{2\Omega_n^2} \qquad (4.18)\\
\frac{d}{dt}\langle P_n P_m\rangle =& -\frac{1}{2}\big\langle\Omega_n^2\{Q_n, P_m\} + \Omega_m^2\{P_n, Q_m\}\big\rangle \\
&- \frac{\Gamma_n + \Gamma_m}{2}\langle P_n P_m\rangle + D_n\frac{\delta_{nm}}{2} \qquad (4.19)\\
\frac{d}{dt}\langle\{Q_n, P_m\}\rangle =& 2\langle P_n, P_m\rangle - 2\Omega_m^2\langle Q_n Q_m\rangle \\
&- \frac{\Gamma_n + \Gamma_m}{2}\langle\{Q_n, P_m\}\rangle \qquad (4.20)
\end{aligned}$$

4.3 Exact solutions

4.3.1 First order

An observant reader may have already noticed that the first order equations (4.13 and 4.14) are analytically solvable. We will first solve these, so that we can understand the results when we move on to the simulations of the moments. We first add the two equations together in such a way as to cancel the Q_n terms (here we will once again leave out the n and ignore the expectation value brackets):

$$\Omega^2\dot{Q} - \frac{1}{2}\Gamma\dot{P} = \Omega^2 P - \cancel{\frac{1}{2}\Gamma Q} + \cancel{\frac{1}{2}\Gamma Q} + \frac{1}{4}\Gamma^2 P = \left(\Omega^2 + \frac{\Gamma^2}{4}\right)P \equiv \omega^2 P \qquad (4.21)$$

Note that we could also solve these differential equations with the standard methods, such as with matrix exponentials. However, for this section and the next, a more explicit strategy was taken because it requires less effort in this specific case. Now we can plug $\Omega^2\dot{Q}$ into the equation for $\dot{P}$, which we get by differentiating equation 4.14:

$$\ddot{P} = -\Omega^2\dot{Q} - \frac{1}{2}\Gamma\dot{P} = -\frac{1}{2}\Gamma\dot{P} - \omega^2 P - \frac{1}{2}\Gamma\dot{P} = -\omega^2 P - \Gamma\dot{P}$$

Putting everything on the left, we can now write down the characteristic equation: $\lambda^2 + \Gamma\lambda + \omega^2 = 0$. Solving this gives $\lambda = \frac{\Gamma}{2} \pm i\Omega$, and so we can find our total solution. The Q_n moment will not be derived, but as it turns out, it solves the exact same differential equation, and so it is of the same form. Here we will also add the indices again:

$$\langle P_n(t)\rangle = e^{-\Gamma_n t/2}(a_n\sin(\Omega_n t) + b_n\cos(\Omega_n t)), \qquad n \in \{1, \ldots, N\} \qquad (4.22)$$
$$\langle Q_n(t)\rangle = e^{-\Gamma_n t/2}(c_n\sin(\Omega_n t) + d_n\cos(\Omega_n t)), \qquad n \in \{1, \ldots, N\} \qquad (4.23)$$

Here a_n, b_n, c_n and d_n are yet to be determined by the initial conditions. We could probably express two of these constants in terms of the other two, but we won't, seen as we'll only be looking at one of these two moments.

4.3.2 Second order

For the second order terms we can also make a few simplifications, and for the terms with $n = m$, we can even find a very neat set of equations. We will begin with the case $n = m$. Let us rename some of our moments: $\sigma^2_{Q_n} \equiv \langle Q_n^2 \rangle$, $\sigma^2_{P_n} \equiv \langle P_n^2 \rangle$, and $R_n \equiv \langle \{Q_n, P_n\} \rangle$. We will also (like usual) drop all the subscripted indices for even more compactness. The moments now look like this:

$$\begin{aligned}
\dot{\sigma}_Q^2 &= -\Gamma\sigma_Q^2 + R - \frac{D}{2\Omega^2} \\
\dot{\sigma}_P^2 &= -\Gamma\sigma_P^2 - \Omega^2 R + \frac{D}{2} \\
\dot{R} &= -\Gamma R + 2\sigma_P^2 - 2\Omega^2\sigma_Q^2
\end{aligned}$$

Now we perform a rather clever (if I may say so myself) trick: we notice that we can cancel the R on the right side if we add $\dot{\sigma}_Q^2$ and $\dot{\sigma}_P^2$ with the right prefactors. In particular, we define two new functions $U = \Omega^2\sigma_Q^2 + \sigma_P^2$ and $V = \Omega^2\sigma_Q^2 - \sigma_P^2$ and find the corresponding set of differential equations:

$$\begin{aligned}
\dot{U} &= -\Gamma U \\
\dot{V} &= -\Gamma V + 2\Omega^2 R - D \\
\dot{R} &= -\Gamma R - 2V
\end{aligned}$$

Let us appreciate for just a moment how amazingly that turned out! We have an analytically solvable differential equation for U (in fact one of the easiest kinds of differential equations), and the other two equations together closely resemble the ones we solved in subsection 4.3.1. The only difference is that now there is an extra constant $-D$ in the equation for V. In any case, let us begin by solving the equation for V:

$$U(t) = U_0 e^{-\Gamma t} \tag{4.24}$$

For the other two equations, we will make a few of the same steps as with the first order equations:

$$2\Omega^2\dot{R} + \Gamma\dot{V} = \cancel{2\Omega^2\Gamma R} - \cancel{2\Omega^2\Gamma R} - 4\Omega^2 V - \Gamma^2 V - \Gamma D = -(4\Omega^2 + \Gamma^2)V - \Gamma D$$

Again, we will plug $\dot{R}$ into $\ddot{V}$:

$$\ddot{V} = 2\Omega^2\dot{R} - \Gamma\dot{V} = -2\Gamma\dot{V} - (4\Omega^2 + \Gamma^2)V - \Gamma D = -2\Gamma\dot{V} - 4\omega^2 V - \Gamma D$$

The characteristic equation for the homogeneous problem is now $\lambda^2 + 2\Gamma\lambda + 4\omega^2 = 0$, which is just the same as before, but with an extra factor 2 before both the Γ and Ω constant. So the homogeneous solution becomes:

$$V_h(t) = e^{-\Gamma t}(a\sin(2\Omega t) + b\cos(2\Omega t))$$

Finding the particular solution of this differential equation isn't difficult: it's simply the constant $-\Gamma D/4\omega^2 = -\Gamma D/(4\Omega^2 + \Gamma^2)$.

$$V(t) = \frac{-\Gamma D}{4\Omega^2 + \Gamma^2} + e^{-\Gamma t}(a\sin(2\Omega t) + b\cos(2\Omega t)) \tag{4.25}$$

Now we want to take a moment to transform back to the moments with which we started. Similarly to last time, we will not derive $R(t)$ here, as it follows a very similar differential equation as $V(t)$. We will also add back the indices for good measure. This goes quite naturally:

$$\begin{aligned}
\left\langle Q_n^2(t)\right\rangle &= \frac{1}{2\Omega_n^2}(U_n + V_n) = \\
&= \frac{1}{2\Omega_n^2}\left(e^{-\Gamma_n t}(U_{n,0} + a_n\sin(2\Omega_n t) + b_n\cos(2\Omega_n t)) - \frac{\Gamma_n D_n}{4\Omega_n^2 + \Gamma_n^2}\right) && (4.26)\\
\left\langle P_n^2(t)\right\rangle &= \frac{1}{2}(U_n - V_n) = \\
&= \frac{1}{2}\left(e^{-\Gamma_n t}(U_{n,0} - c_n\sin(2\Omega_n t) - d_n\cos(2\Omega_n t)) + \frac{\Gamma_n D_n}{4\Omega_n^2 + \Gamma_n^2}\right) && (4.27)\\
\langle\{Q_n, P_n\}(t)\rangle &= \frac{-2D_n}{4\Omega_n^2 + \Gamma_n^2} + e^{-\Gamma_n t}(e_n\sin(2\Omega_n t) + f_n\cos(2\Omega_n t)) && (4.28)
\end{aligned}$$

All of these equations are valid for $n \in \{1, \ldots, N\}$. Again, the constants $a_n, \ldots, f_n$ can be determined with the initial conditions. To put into words what these equations mean: the variances of the position and momentum operators are a decaying (exponential) term added to an exponentially decaying sinusoidal added to a constant shift.

One thing we need to consider is the requirement that variances are always positive. Is this requirement met by the solutions as given in equations 4.26 and 4.27? As it turns out, it is *not*. If we look at the limit of $t \to \infty$ for $\langle Q_n^2(t)\rangle$, we see that the limit is negative. This is not a good thing. In practice, that constant will often be very small compared to the other term, but the fact remains that the variance in the limit equals a negative constant. How it is possible that this constant is negative is unknown; further research is required to discover which approximation leads to this. Interestingly, in this supplementary info [12], equation 4.18 contains a plus sign, instead of a minus sign; that would lead to a positive constant.

We want to also take a quick look at what happens for $t \to \infty$ when $\Gamma_n = 0$: we see that the variance then oscillates like a sinusoidal (with an added constant).

For the case $m \neq n$ (the cross-correlations), we cannot make quite the same simplifications as we did for $m = n$; the result of this is that we will not solve this case analytically and that the graphs of those are also going to turn out a little more intricate.

5 Results

In this section, we display all the output resulting from the simulations of some of the equations that we saw in the previous sections. We will begin with the simulation of the Lindblad master equation (3.1), from which we can calculate the density matrix and the moments (using 3.3) directly. Consequently, we will calculate those same moments using the differential equations described in section 4.2; we will solve those differential equations numerically and hopefully see the similarity with the first approach.

5.1 Density matrix

In a Python program, a simulation of the Lindblad master equation was run for $N = 3$ and $s = 11$, using RK4, the classic Runge-Kutta method. The network that was used is the m_2 network, a.k.a. the chain with three nodes. We also take $D_n = 0$ for all n, and simulate 150 steps over a duration of 7.5 seconds. As initial conditions, a density matrix was created with expectation values 0 for all the momenta, and for the position operators: $(\langle Q_1 \rangle, \langle Q_2 \rangle, \langle Q_3 \rangle) = (0.1713, 0.1515, 0.1373)$. The result is shown in figure 3.

The graphs of the solutions (in color) seem to come very close to the expected solution (dotted black line). The expected solution was calculated by equation 4.13. The reason for the deviation in the graph of mode 1, which becomes more prominent near the end of the graph, is due to the instability caused by implementing a maximal state number. The number of steps (150) is also relatively low; this was done to suppress the running time of the program, which is not to be underestimated for $s = 11$. To make this simulation more accurate, it might be advisable to get a more powerful computer than the laptop that was used in this project, or to use some kind of simplifications or optimizations to allow for larger s and larger dt without costing too much time.

Nonetheless, one can see that for low Γ_n, the simulation is very close to the expectation, and even for higher Γ_n, it closely approximates the expected graph. To get a better idea of how closely they resemble, we plot the graphs of the difference between the found and expected solution, divided by the maximum value that the expected solution attains, similarly to a relative error. This is shown in figure 4.

The errors for $\langle Q_2 \rangle$ and $\langle Q_3 \rangle$ look quite nice (if it's even possible to say an error looks nice); they follow an increasing sinusoidal with the same frequency as the original graphs. The error in $\langle Q_1 \rangle$ is a lot less predictable; this is most probably a consequence of the fact that Γ_1 is considerably larger than Γ_2 and Γ_3.

5.2 Moments

Again in Python, a different simulation was run to see visually how the differential equations for the moments play out, in the first order (4.13, 4.14), and in the second order (4.18 - 4.20). Using the RK4 once again, the solution to the differential equations were numerically approximated. Because this simulation is considerably

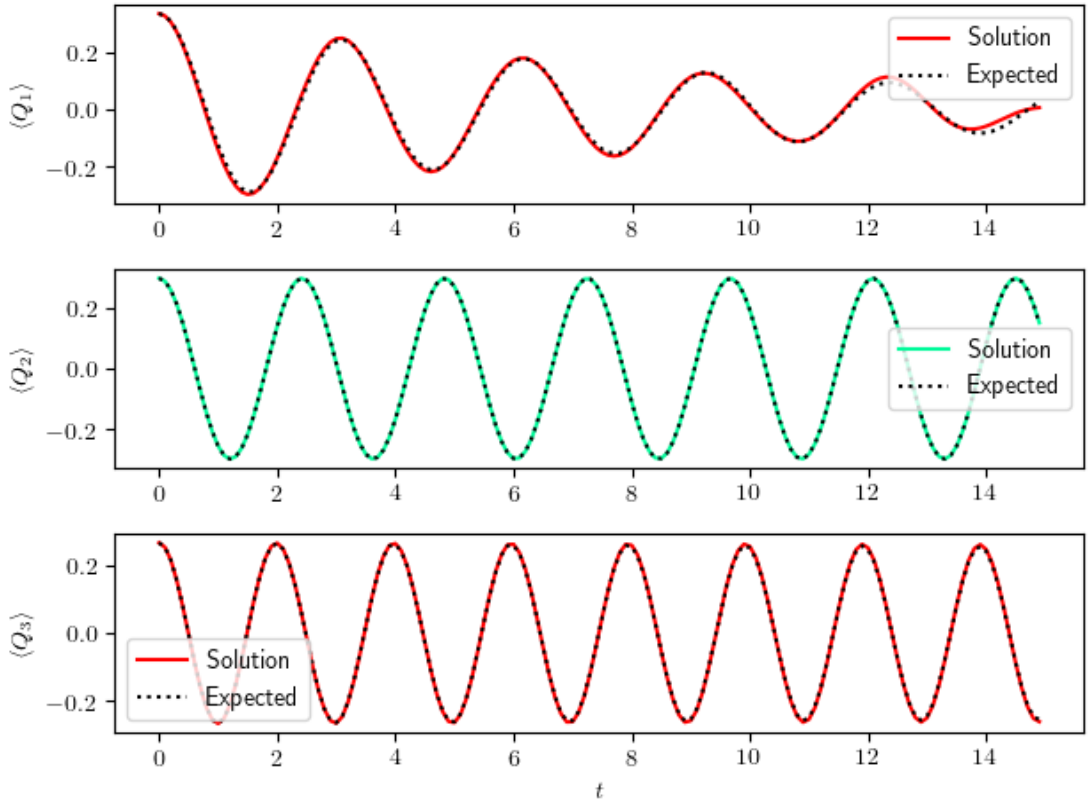

Figure 3: *The moments of the position operators in the mode basis of the m_2 (chain) network, as obtained by solving the Lindblad master equation (3.1) under the following assumptions: the maximal state number for each oscillator is $s = 11$, and $D_n = 0$. The simulation was run for t ranging between 0 and 7.5 seconds, with 150 steps. Also shown is the expected solution, as calculated by equation 4.13.*

lighter on the computer, several networks were investigated, with various sets of parameters. The code for these is also given in section A of the appendix.

5.2.1 First order, homogeneous ω

First, we look at the network m_2, the chain with $N = 3$ nodes, initially considering only the first order moments. For the initial conditions we take $(\langle p_1 \rangle, \langle p_2 \rangle, \langle p_3 \rangle, \langle q_1 \rangle, \langle q_2 \rangle, \langle q_3 \rangle) = (0.5, 1, -1, -1, 0, 1)$, and we set $1 = \omega_1 = \omega_2 = \omega_3$, and $\gamma = 0.07\omega_2$. Notice that the initial conditions are all in the node basis. We also use a time scale from 0 to 75 seconds, and 15000 steps within that time frame. The results of this simulation are shown in figure 5.

What do we see here? That there is one noiseless mode (mode 2, as we expected) and that one of the nodes (node 2, this is a coincidence) synchronizes very quickly. The other modes are subject to noise, and especially mode 3, which isn't noiseless but has a long decay time, causes node 1 and 3 to exhibit the behavior of a beat tone, i.e. two frequencies superposed onto each other. This eventually becomes a single frequency in the high limit for t. Furthermore, although node 2 seems to be

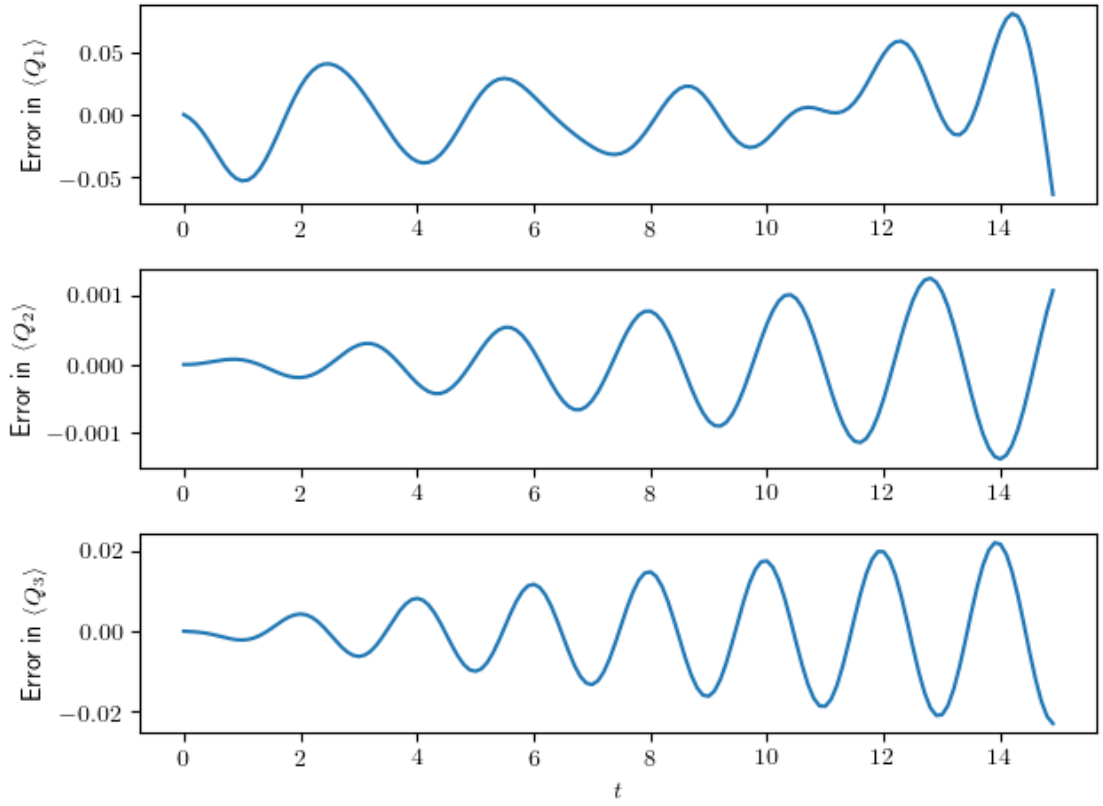

Figure 4: *The error in the moments of the position operators in the mode basis of the m_2 (chain) network relative to the maximum of the expected solution. The same assumptions and parameters were used as for the previous image.*

more coherent than node 1 and 3, it is actually the one which dies down in the limit as $t \to \infty$. A graph to prove these last two claims can be found in figure 11 of the appendix, section C.

To get a better idea of the ratios of the between the decay times of the nodes, we can look at the factor Γ_i:

$$\Gamma = \gamma((\mathcal{F}_{1i} + \mathcal{F}_{2i} + \mathcal{F}_{3i})^2, i \in \{1,2,3\}) = 0.07\omega_2 \begin{pmatrix} (1+\frac{\sqrt{2}}{2})^2 \\ 0 \\ (1-\frac{\sqrt{2}}{2})^2 \end{pmatrix} = 10^{-3} \begin{pmatrix} 203.995 \\ 0 \\ 6.005 \end{pmatrix}$$

So the third mode decays around 34 times slower than the first mode; this follows from the exact solution of the differential equation in 4.23.

5.2.2 First order, inhomogeneous ω

Now it might be interesting to look at what changes when the node frequencies are different with respect to each other. We set $1 = \omega_2 = \omega_1/1.2 = \omega_3/1.8$, similarly to [13], and keep all other parameters the same. The result of this is shown in figure 6.

What we see here in a way resembles figure 5, and in a way also differs. There are now no more noiseless modes, which means that in the end, all the nodes will

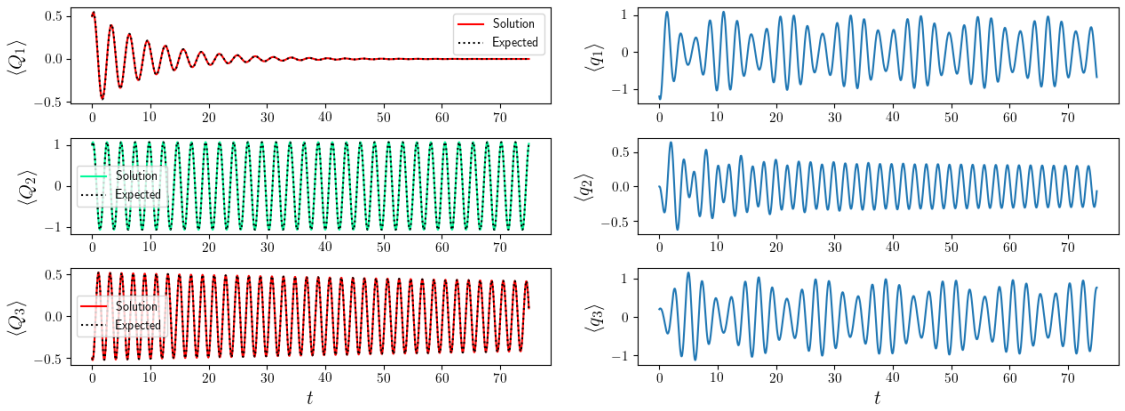

(a) ***(b)***

Figure 5: *A simulation of the first order moments of the position operators in the m_2 (chain) network. An set of graphs is included both for the normal mode basis* ***(a)*** *— where the red graphs are subject to noise, but the light green graph is noiseless — and in the original (node) basis* ***(b)****. Both are shown as a function of time; 15000 steps were taken over a duration of 75 seconds.*

decohere. The reason for this is that with a non-constant ω, the eigenspace of the adjacency matrix and that of the system Hamiltonian no longer coincide, and so the noiseless eigenvector that we found in the simple case is no longer necessarily noiseless.

What we do see, however, is that node 2 decays very slowly; in fact, if we calculate Γ (numerically) for this case, we will find

$$\Gamma = 10^{-1} \begin{pmatrix} 1.5402 \\ 0.0605 \\ 0.4993 \end{pmatrix}$$

This time, the ratio of Γ_2 over the maximum (Γ_1), is around 1/25. We will consider this mode to be *quasi-noiseless*. The existence of a quasi-noiseless mode implies the possibility for nodes to stay coherent for a long time, even if not forever. Both node 1 and 2 are an example of this; they appear to stay coherent for the full 75 seconds.

5.2.3 Second order, homogeneous ω

We will go one step further and also investigate the correlations between Q_n and Q_m. For that we have also simulated equations 4.18, 4.19 and 4.20. We would like to find out several things: do the results of the simulation match up with the theoretical predictions we made in subsection 4.3.2? How does a mode being noiseless affect the behavior of the variances? These questions will be answered in this subsection.

Using the same program as last time (with some modifications), a simulation was run to find the correlations of the position operators in the mode basis. Once again, we look at the m_2 network. In order to answer the first question, we will plot $U_n = \langle \Omega_n^2 Q_n + P_n \rangle$ for $n \in \{1, 2, 3\}$. We use the idealized case with $1 =$

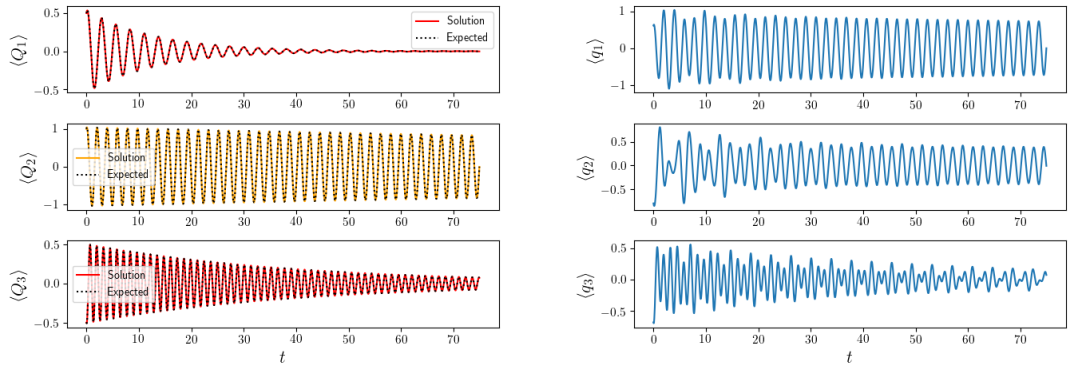

(a) ***(b)***

Figure 6: *A simulation of the first order moments of the position operators in the m_2 (chain) network. Again, the normal modes are shown in* ***(a)*** *— this time there is a new color: orange, which represents a quasi-noiseless mode — and the node basis in* ***(b)****. Both are shown as a function of time; again, 15000 steps were taken over a duration of 75 seconds.*

$\omega_i, \forall i \in \{1,2,3\}$. For initial conditions, we take $\langle P_n^2(0) \rangle = 1, \forall i \in \{1,2,3\}$, and $\langle (P_1 P_2)(0) \rangle = -\langle (P_1 P_3)(0) \rangle = -\langle (P_2 P_3)(0) \rangle = -1$. We also have a new parameter, the temperature of the bath T; this we set to $T = 10\omega_2$. The result of this plot is shown in figure 7a.

In this image, the solid colored lines are the solutions obtained by RK4, applied to the differential equations. The dotted black lines are the analytic solutions of equation 4.24. Aside from making it unlikely that mistakes were made in the derivation of subsection 4.3.2, figure 7a isn't very interesting, so let's move on to the actual moments that we care about. They are shown in the grid in figure 7b. One can see here that the variances of each mode subject to noise, decays. All the cross-correlations disappear in the end. That is not necessarily the case; in the case of the m_3 network, there are two noiseless modes, and the cross-correlation between them does not disappear (this is shown in subsection B of the appendix).

We want to take a slightly more detailed look at each of the second order moments. Therefore, all six simulations have been shown again in figure 8.

Here you can see that for the modes with noise, the variances also decay to zero, whereas the variance of the noiseless mode is periodic without decay. For the cross-correlations, we also see some interesting behavior; the cross-correlation between Q_1 and Q_2 dies out very quickly, and similarly for the correlation between Q_1 and Q_3, but the one between Q_2 and Q_3 doesn't visibly die out within the scope of this simulation. However, when running the simulation for much longer (around 900 seconds), it becomes clear that it also decays (this image has been included in section C of the appendix, see figure 13). In the case of the $m = 3$ network, which has two noiseless modes, the cross-correlation between those does not die out, as can be seen in figure 10b.

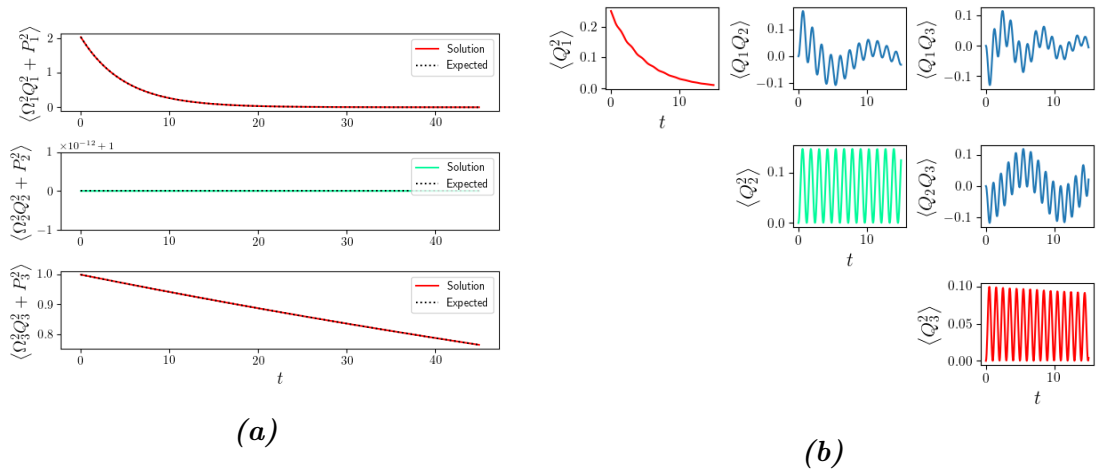

(a) *(b)*

Figure 7: ***(a)*** *A simulation of the moment $U = \langle \Omega_n^2 Q_n + P_n \rangle$ in the m_2 (chain) network (in color), as a function of t, ranging from 0 to 45 in 15000 steps. The shown graphs are all exponentials, as the expected graphs (black dotted line) perfectly match the solutions. Since mode 2 is noiseless, its graph is a constant 1 (an exponential, starting at 1, with no decay). Also shown is* ***(b)****, the auto- and cross-correlations of the moments of the position operators, as a function of t. This time, t goes from 0 to 15, to prevent the images from becoming cluttered.*

5.3 Discussion

We would like to shortly discuss the results that we have acquired to investigate whether they meet our expectations, beginning with figures 3. We can see that the simulated graph closely approximates the expected solution that we calculated explicitly, although looks are slightly deceiving here; we can see from the relative error graph in figure 4 that the error is not insignificant, even in the very beginning. The reason for the instability is, as said, attributed to the cutoff; this is supported by the fact that the positivity of the density matrix is always lost at the same point in time for the same network parameters and the same s. That is, changing the time interval dt — as long as it is not too large — has no effect on the time at which ρ is no longer positive. That is why, in these simulations, the full time interval had to be taken smaller. It is also why the only assertion made in this simulation was that *one* iteration preserves the positivity of ρ. The unit trace and Hermitian property were at all times preserved.

We also look at figure 5. For the mode graphs (5a), we can say that they indeed look as we expected; two of the nodes decay, and one mode is noiseless, just like we saw in section 2.1. For the node graphs (5b), we expect the noiseless mode $\frac{\sqrt{2}}{2}(1, 0, -1)$ to span the first and third component; for $t < 75$ this is not yet quite evident, but figure 11 shows that indeed, node 2 decays, whereas node 1 and 3 synchronize in the limit.

In figure 6, the assumption we did in section 2.1 that $\omega_i = \omega$ clearly breaks down, and so does the noiseless mode. What we do see is that the relative Γ's are somewhat preserved; mode 1 decays the fastest, then mode 3, and finally mode 2. Since we don't have the noiseless cluster $\frac{\sqrt{2}}{2}(1, 0, -1)$ anymore, we don't know *a*

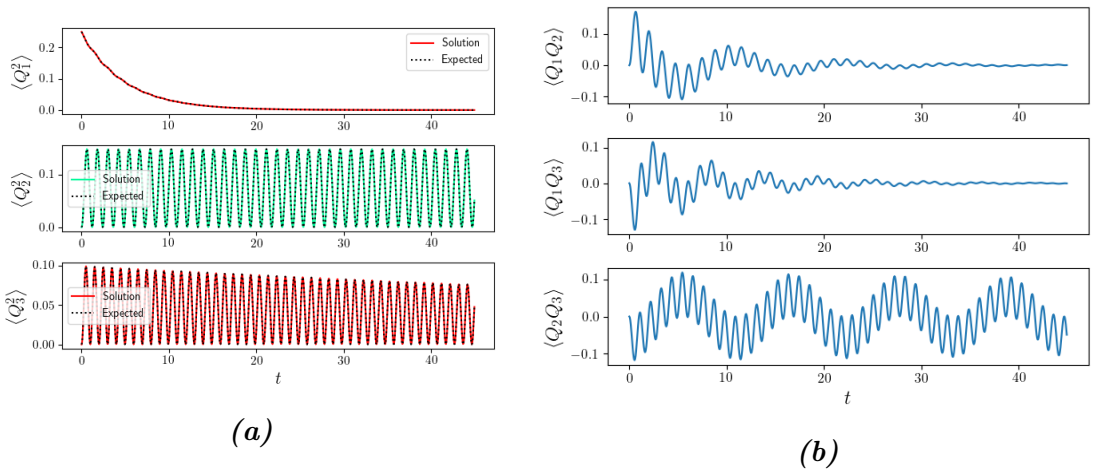

Figure 8: ***(a)*** *A simulation of the variances of the position operator $\langle Q_n^2 \rangle$ in the m_2 (chain) network, as a function of t, ranging in 15000 iterations from 0 to 45. This time, the expected graphs were omitted, seen as they once again perfectly matched the solution to the differential equations. Also shown is* ***(b)****, the cross-correlations of the position operators, as a function of t, with the same settings as in* ***(a)****.*

priori which nodes will stay synchronized for the longest; as it turns out, they are 1 and 2; this can already be seen in 6b, and is shown in greater detail in figure 12 in section C of the appendix.

Now we move on to the second order, homogeneous ω network. As we could see, the U graph looks perfectly as expected (in figure 7a), and so do the variances of the position operators (in figure 8a). With the right initial conditions, they seem to stay positive although in reality they tend to a negative constant (as the theory predicts). These graphs make it evident once again that mode 2 is the only noiseless mode, as the variances of the other decay to a constant. For the cross-correlations, we see (figure 13) that all of the cross-correlations decay to zero; this can also be expected, as there is only one noiseless mode. Specifically, they are all the correlation between a noiseless mode (which does not decay) and a mode that is subject to noise (which does decay) or between two noisy modes. And we know that such a correlation is condemned to evanescence.

So it seems that all the results for the moments simulations based on the assumption of Gaussian states can be understood and explained, aside from the negative limit for long durations.

6 Conclusion

What can we conclude from all of these results? The first conclusion, going back to section 2, is that noiseless clusters are most prevalent for probabilities close to either 0 or 1; that is, when the networks are either highly connected or highly disconnected.

Furthermore, we conclude that it is much more efficient and sensible to calculate the differential equations for the moments, and then simulate those, rather than simulation the full Lindblad master equation. This is because the simplified approach gives the expected results, which can be fully explained by the knowledge of noiseless clusters that we built up in section 2. In fact, the graphs of the simpler approach are more stable than the graphs of the full simulation. Furthermore, it doesn't require simulation the full density matrix, which consists of very many elements even for a very humble choice of node count N and maximal state s, whereas for the simplified approach, only one number per desired moment suffices to contain all the necessary information.

Also, the simulation of the second order moments was not possible using the direct simulation because of the instabilities cause by cutting of the matrices at finite values. A suggestion for further research could therefore be to investigate methods to stabilize the the terms of the Lindblad master equation with the D_n as a prefactor. An alternative to manually simulating the Lindblad master equation is to use [14] or by solving the Fokker-Planck equations [15].

From the simulation of the moments only, we can conclude that the existence of noiseless modes does indeed follow from the Lindblad master equation, and that exactly those modes which we expected to be noiseless are noiseless. One thing that is still unclear is why the theory predicts (and the simulations confirm) that the position variances tend to a negative constant in the limit of $t \to \infty$. This might also require more investigation, namely to find out where this sign comes from, whether it's a mistake or a result of an approximation in the derivation of the Lindblad master equation.

References

[1] Peter W. Shor. Polynomial-time algorithms for prime factorization and discrete logarithms on a quantum computer. *SIAM Journal on Computing*, 26(5):1484–1509, oct 1997. doi: 10.1137/s0097539795293172.

[2] Abhilash Ponnath. Difficulties in the implementation of quantum computers. *CoRR*, abs/cs/0602096, 2006. URL http://arxiv.org/abs/cs/0602096.

[3] Quantum decoherence, . URL https://en.wikipedia.org/wiki/Quantum_decoherence.

[4] Daniel A. Lidar and K. Birgitta Whaley. Decoherence-free subspaces and subsystems. In *Irreversible Quantum Dynamics*, pages 83–120. Springer Berlin Heidelberg, 2003. doi: 10.1007/3-540-44874-8_5.

[5] H. Scutaru A. Sandulescu. Open quantum systems and the damping of collective modes in deep inelastic collisions. 173(2):277–317, feb 1987. doi: 10.1016/0003-4916(87)90162-x.

[6] A. Cabot, F. Galve, V.M. Eguíluz, K. Klemm, S. Maniscalco, and R. Zambrini. Unveiling noiseless cluster in complex quantum networks. *Nature Partner Journals*, 2018.

[7] J. D. Hunter. Matplotlib: A 2d graphics environment. *Computing in Science & Engineering*, 9(3):90–95, 2007. doi: 10.1109/MCSE.2007.55.

[8] D. Manzano. *A short introduction to the Lindblad Master Equation*. University of Granada. E-18071 Granada. Spain.

[9] Heinz-Peter Breuer and F. Petruccione. *The theory of open quantum systems*. Oxford University Press, 2010.

[10] Open quantum systems/the quantum optical master equation, . URL https://en.wikiversity.org/wiki/Open_Quantum_Systems/The_Quantum_Optical_Master_Equation.

[11] R. E. Edwards. Positive definite functions and bochner's theorem. In *Graduate Texts in Mathematics*, pages 148–154. Springer New York, 1979. doi: 10.1007/978-1-4612-6208-4_9.

[12] G. Manzano, F. Galve, G.L. Giorgi, E. Hernández-García, and R. Zambrini. Supplementary information for "synchronization, quantum correlations and entanglement in oscillator networks". *Scientific Reports*, 2013.

[13] Gonzalo Manzano, Fernando Galve, Gian Luca Giorgi, Emilio Hernández-García, and Roberta Zambrini. Synchronization, quantum correlations and entanglement in oscillator networks. *Sci Rep*, 3(1):1439, mar 2013. doi: 10.1038/srep01439.

[14] J.R. Johansson, P.D. Nation, and Franco Nori. QuTiP 2: A python framework for the dynamics of open quantum systems. *Computer Physics Communications*, 184(4):1234–1240, apr 2013. doi: 10.1016/j.cpc.2012.11.019.

[15] Viktor Holubec, Klaus Kroy, and Stefano Steffenoni. Physically consistent numerical solver for time-dependent fokker-planck equations. *Phys. Rev. E*, 99 (3):032117, mar 2019. doi: 10.1103/physreve.99.032117.

Appendix

A Code

The code for all of the simulations which were run over the course of this project are included in this GitHub repository, specifically in the subfolder *Python*. The simulation that generated figure 2 is in *NoiselessSubsystems.py*, for figure 14 in *NoiselessSizes.py*. Both of those files also use code from the file *common.py*. The simulations of the moments can be found in *DensitySims.py* and *MomentSims.py*, for the direct (Lindblad) simulation and for the simplified (Moments only) simulation, respectively. These last two files also implement *moments_common.py* for the definitions of many constants, some functions, and the RK4 integration routine and *moments_plotter.py* to generate the figures. The density simulations also use *operators.py* for the definitions of all the P_n and Q_n operators, the superoperators, the (anti)commutator and *density_initial.py* for the initial conditions of ρ.

The repository contains other directories as well; for example, *JARs* contains the Java program which was made to generate the images in figure 1. *Images* contains all the images of this paper and more. Finally, *Maple* contains two related Maple worksheets; one of those was used to diagonalize some of the adjacency matrices, and the other was used to demonstrate that cutting off the position and momentum operator leads to an instability in their commutator (equation 4.7).

B Moments of the m_3 network

Simulations were also run for the m_3 network to compare the two networks. Initially, the simulation was run with constant parameters ($\omega_1 = \omega_2 = \omega_3 = 1$), and with the same initial conditions as in the first order homogeneous case (5.2.1): $(\langle p_1\rangle, \langle p_2\rangle, \langle p_3\rangle, \langle q_1\rangle, \langle q_2\rangle, \langle q_3\rangle) = (0.5, 1, -1, -1, 0, 1)$ and $\gamma = 0.07\omega_2$.

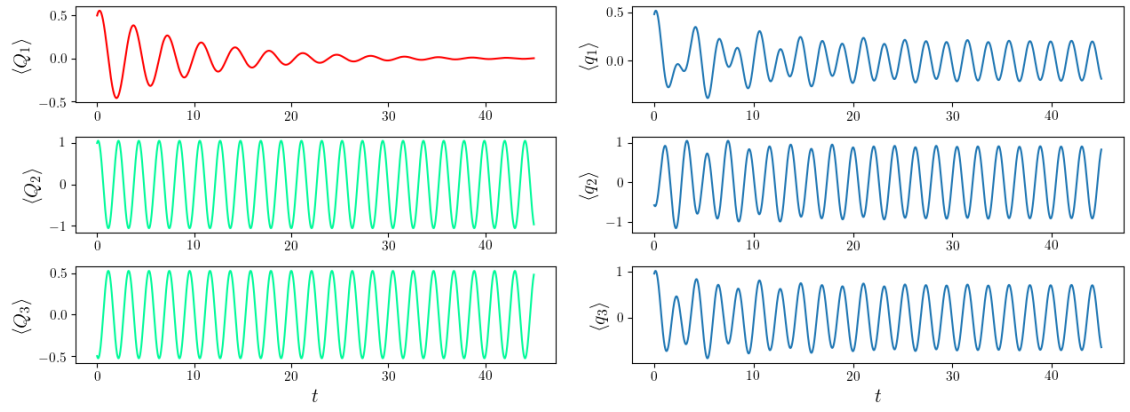

(a) ***(b)***

Figure 9: *The first order moment simulations for the m_3 network in the mode basis* ***(a)*** *and in the node basis* ***(b)****. Now there are two noiseless modes which span all three nodes of the graph. Once again, time ranges from 0 to 45 in 15000 steps.*

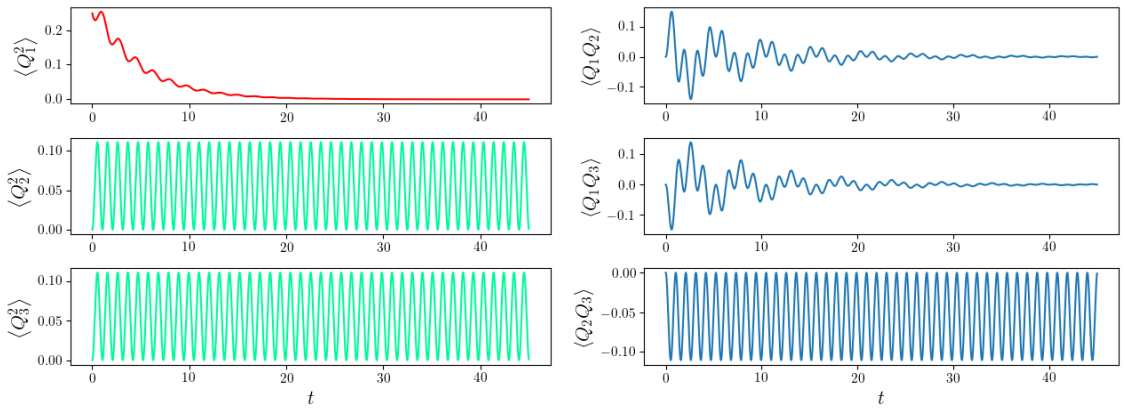

(a) ***(b)***

Figure 10: ***(a)*** *A simulation of the variances of the position operator $\langle Q_n^2 \rangle$ in the m_3 (triangle) network, as a function of t, ranging in 15000 iterations from 0 to 45 and* ***(b)****, the cross-correlations of the position operators, as a function of t, with the same settings as in* ***(a)****.*

C Decay of the moments

Several of the operator moments have been claimed to be subject to decay, but don't visually decay in the time period of the simulation. Therefore, a set of images has been included for a longer range of values of t. For example, in section 5.2.1 was claimed that node 2 decays, whereas node 1 and 3 eventually synchronize. An image to support this claim can be found in figure 11. Also, in section 5.2.2 was said that all nodes decay; the graph in figure 12 supports this claim. Finally, in section 5.2.3, it was mentioned that the cross-correlation between Q_2 and Q_3 also decays, despite there not being any visual indication that this is indeed true. Therefore, another image has been included in figure 13. These images can all be found on the next page.

D Extra information on noiseless clusters

Connectedness

Going back to the analysis of networks that we performed in 2, we might also be interested in the quantity of connected components in each network, to get an idea of the type of networks which contain NSs. We want to state and prove the following theorem about the number of connected components in a graph, and consequently we want to apply this theorem to count the number of connected components in a graph which contains a NS. The theorem is as follows:

Theorem 1. *For an arbitrary graph G, the number of connected components s is equal to the dimension of the null space of the Laplacian matrix L:*

$$s = \dim \mathrm{Null}(L)$$

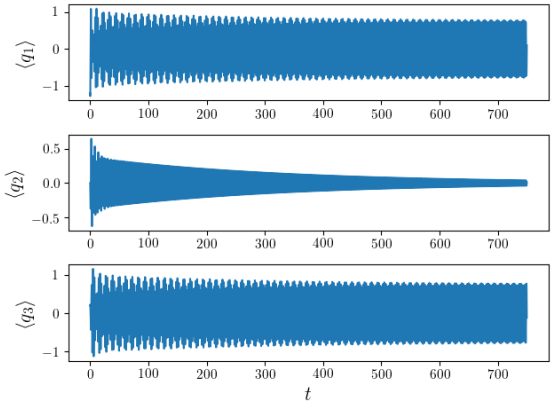

Figure 11: *The same simulation as 5b, but now with t increasing in 15000 steps from 0 to 750. Indeed, the second node vanishes for large t, and the first and third node slowly converge to a single sinusoidal.*

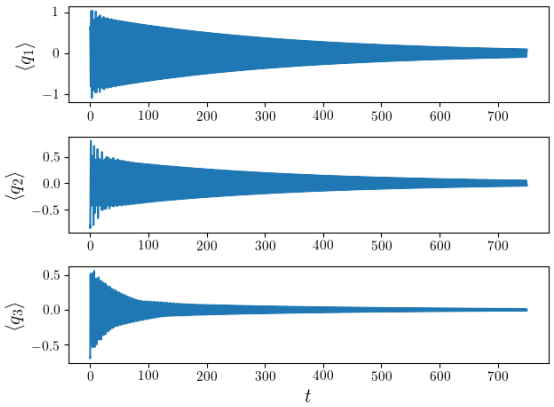

Figure 12: *The same simulation as 6b, but now with t increasing in 15000 steps from 0 to 750. Now all nodes vanish for large t, but the first and second node decay the slowest.*

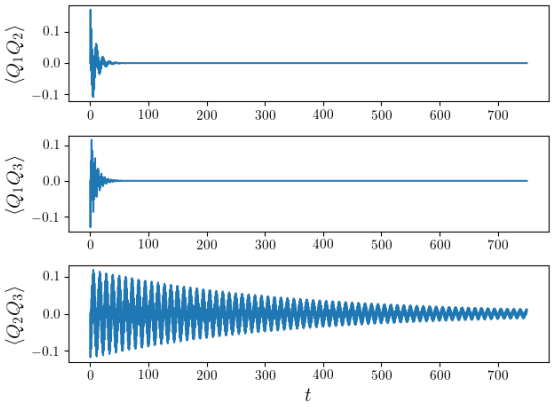

Figure 13: *The same simulation as 8b, but now with t increasing in 15000 steps from 0 to 700. Indeed, the third cross-correlation decays.*

Let's prove this. We will begin with a definition to make the proof easier.

Definition 6.1. A subgraph G_1 of G will be called isolated when

$$\forall i \in G.N \setminus G_1.N : \forall j \in G_1.N : L_{ij} = L_{ji} = 0$$

Here $G_1.N$ is the set of nodes of G_1. ($L_{ij} = L_{ji}$ is always the case, this follows from the symmetry of the adjacency matrix.)

Intuitively: there are no connections between G_1 and the nodes outside of G_1. With that definition, the following theorem will become easier to prove:

Theorem 2. *Let G_1 a subgraph of G which is isolated within G. Enumerate the nodes $G.N$: $1, \ldots, n$. Take the vector $\mathbf{a}$ with elements*

$$a_i = 1_{G_1.N}(i) = \begin{cases} 1, & i \in G_1.N \\ 0, & otherwise \end{cases}$$

Then the following holds: $L\mathbf{a} = \mathbf{0}$. The converse is also true: $L\mathbf{a} = \mathbf{0} \implies G$ is isolated.

Proof. " $\implies$ ": we look at the i-th component of $L\mathbf{a}$;

$$[L\mathbf{a}]_i = \sum_n L_{ni} a_i$$

Now we see immediately for $i \in G.N \setminus G_1.N$ that $a_i = 0$, so from now on we assume that $i \in G_1.N$. Then we get:

$$[L\mathbf{a}]_i = \sum_{n \neq i} L_{ni} a_n - d_i a_i = \sum_{n \neq i} L_{ni} a_n - \sum_{n \neq i} L_{ni} \cdot 1 = \sum_{n \in G_1.N \setminus \{i\}} L_{ni} \cdot 1 - L_{ni} = 0$$

" $\impliedby$ ": we use the contraposition. Assume $\exists i \in G_1.N : \exists j \in X = G.N \setminus G_1.N : L_{ij} = L_{ji} \neq 0$. Then for component i of $L\mathbf{a}$ it holds that:

$$\begin{aligned} [L\mathbf{a}]_i = \sum_n L_{ni} a_n &= \sum_{n \neq i} L_{ni} a_n - L_{ni} \cancelto{1}{a_i} \\ &= \sum_{n \in G_1.N \setminus \{i\}} L_{ni} - L_{ni} + \sum_{n \in X \setminus \{i\}} -L_{ni} \\ &= \sum_{n \in X \setminus \{i\}} -L_{ni} \leq -L_{nj} = -1 < 0 \end{aligned}$$

So $L\mathbf{a} \neq \mathbf{0}$, so the converse has also been proven. □

We now know that a component is isolated $\iff$ we can find a "special vector" in the null space of L. Furthermore, for two subgraphs of G it holds that those "special vectors" are orthogonal $\iff$ the two subgraphs are disjoint: this follows trivially from the definition of those special vectors (if there is a component for which those "special vectors" are both unequal zero, then the nodes of those subgraphs are automatically not disjoint). Now the proof of theorem 1 follows almost directly from this observation.

Cluster sizes

We might also want to investigate the sizes of clusters in which we can find noiseless clusters. In order to do that, we count the number of noiseless clusters for each NS size and each component size out of the total of 5000 tries, and, using the parameters $N = 15$, $p = 0.05$, we got to the image displayed in figure 14.

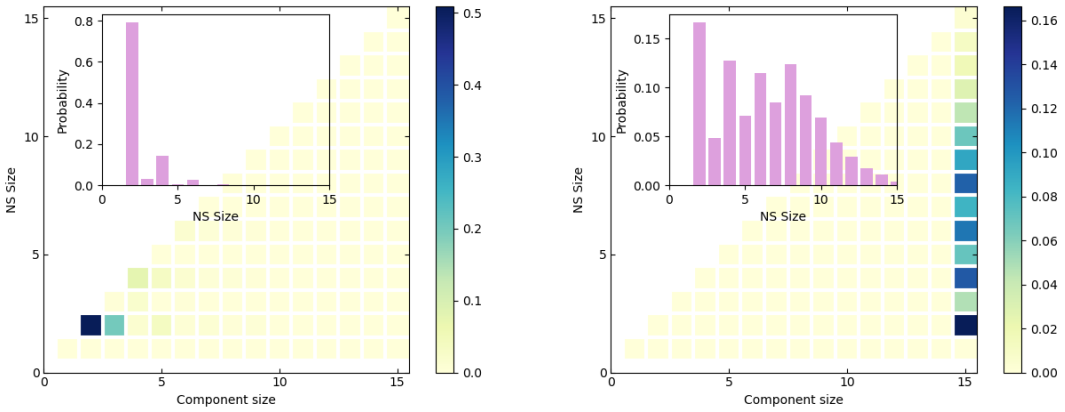

(a) ***(b)***

Figure 14: *The number of times a noiseless cluster was found for each value of the component size and the NS size, both ranging from 1 to 15, out of 5000 Erdos-Renyi networks with* $N = 15$*. For the probability of connection we chose* $p = 0.05$ *in* ***(a)*** *and* 0.80 *in* ***(b)****. It's meant to be similar to figure 3 in [6], but it's not quite the same.*

This image doesn't look quite like it should yet, according to figure 3 in [6], and it was included simply for the sake of completeness.